Russian Journal of Herpetology Vol. 23, No. 3, 2016, pp. 163 – 194

CONTRIBUTION TO THE HEAD ANATOMY OF THE BASAL FROG *Barbourula busuangensis* AND THE EVOLUTION OF THE ANURA

Zbyněk Roček,[1] Natalia Baleeva,[2] Anne Vazeille,[3] Alberto Bravin,[4] Eddie van Dijk,[5] Christian Nemoz,[4] Tomáš Přikryl,[1] Ella M. Smirina,[6] Renaud Boistel,[3] and Leon Claessens[7]

Submitted May 2, 2016

Barbourula busuangensis Taylor and Noble, 1924 is a poorly known basal aquatic frog from the Philippines. Here we describe some features of the head anatomy of *B. busuangensis*, with a focus on jaw and eye musculature and the cranial skeleton, based on 3D reconstructions from serial histological sections of a metamorphosed but not fully grown (subadult) female and two fully grown adults, one of which was investigated by synchrotron x-ray imaging. Examination of two different post-metamorphic stages allowed tentative assessment of the development of some characters from the subadult to the adult condition, e.g., shape and size of the parahyoid or arrangement of some jaw adductors. The subadult specimen of *B. busuangensis* also possesses some unique cranial characters, including a salamander-like arrangement of the jaw adductors, which is obscured in fully grown adults, and a well-developed basal (= basicranial) articulation resembling that of temnospondyls. The facial nerve of *B. busuangensis* does not fuse with the trigeminal ganglion. Head anatomy confirms that *Barbourula* is a basal anuran, and comparison with other basal taxa suggests that *B. busuangensis* most closely resembles the hypo-ossified taxa *Alytes* and *Bombina*, and *Discoglossus* with respect to degree of ossification.

Keywords: Anura; *Barbourula*; *Liaobatrachus*; head anatomy; evolutionary trends; relationships; cranium; palatoquadrate; cranial nerves; jaw adductors; extrinsic eye muscles.

INTRODUCTION

The genus *Barbourula* contains two species, *B. busuangensis* Taylor et Noble, 1924 and *B. kalimantanensis* Iskandar, 1978, which are endemic to Palawan and Borneo, respectively. The genus is considered to be closely related to *Bombina* and *Discoglossus* (Taylor and Noble, 1924; Myers, 1943; Inger, 1954; Sanchiz, 1984; Clarke and Cannatella, 1993; Ford and Cannatella, 1993; Iskandar, 1995; Blackburn et al., 2010). Based on molecular evidence, Blackburn et al. (2010) suggested that *Barbourula* diverged from *Bombina* in the Paleogene, and that both *Barbourula* species diverged from one another in the Late Miocene. The earliest fossil material of *Bombina* is from the Early Miocene of Germany (Sanchíz and Schleich, 1986) and thus the divergence time between *Bombina* and *Barbourula* cannot be confirmed by paleontological data. Early Eocene anuran fossil material from India, represented by ilia, vertebrae and urostyles, may be related to *Barbourula* (Folie et al., 2013).

Barbourula specimens are relatively rare in museum collections, but additional specimens have been collected in the last decade (e.g., Bickford, 2008; Blackburn et al., 2010); due to its relative rarity, few morphological accounts have been published. There are a few osteological notes on *B. busuangensis* (Taylor and Noble, 1924; Trueb, 1973; Iskandar, 1978), and a description of the skeleton by Clarke (1987). Pelvic and thigh muscles in *B. busuangensis* were described by Přikryl et al. (2009). *Barbourula kalimantanensis* is, besides *Telmatobius cu-*

[1] Department of Palaeobiology, Geological Institute, Czech Academy of Sciences, Rozvojová 136, CZ-165 00 Prague 6, Czech Republic.

[2] Department of Vertebrate Zoology, St. Petersburg State University, Universitetskaya nab. 7/9, St. Petersburg, 199034 Russia.

[3] Institut International de Paléoprimatologie et de Paléontologie Humaine, Université de Poitiers, Poitiers, France.

[4] European Synchrotron Radiation Facility (ID17), 6 Rue Jules Horowitz, 38000 Grenoble, France.

[5] Department of Botany and Zoology, Stellenbosch University, Private Bag X1, Matieland, 7602 South Africa.

[6] Laboratory of Postnatal Ontogeny, Koltzov Institute of Developmental Biology, Russian Academy of Sciences, Vavilova 26, Moscow, 119334 Russia.

[7] Department of Biology, College of the Holy Cross, 1 College Street, Worcester, MA 01610, USA.

leus from lake Titicaca, the only other known frog that has strongly reduced lungs (Bickford et al., 2008; Hutchinson, 2008). Tadpoles are unknown.

Barbourula is of special interest because osteologically it resembles *Liaobatrachus*, an Early Cretaceous anuran from China (Roček et al., 2012; Dong et al., 2013). Both *Liaobatrachus* and *Barbourula* have an elongated frontoparietal fontanelle, exhibit similar configurations of the maxilla and the maxillo-premaxillar contact, the parahyoid, and possess free ribs with uncinate processes, the shapes and positions of which are identical between both taxa. *Liaobatrachus* and *Barbourula* both possess broadly dilated sacral diapophyses, and a urostyle with a pair of transverse processes. However, the shapes of the vertebral centra and the numbers of presacral vertebrae differ between both taxa (Clarke, 1987; Roček et al., 2012). For phylogenetic placement of *Barbourula* among archaeobatrachian frogs see Cannatella (1985), Gao and Wang (2001), Blackburn et al. (2010), Pyron and Wiens (2011), and Dong et al. (2013).

Based upon serial histological sectioning of a metamorphosed but not fully developed (subadult) individual, synchrotron x-ray examination of a fully developed individual and anatomical analysis of a second adult specimen, here we provide new information on the mandibular adductor musculature in *Barbourula*, its extrinsic eye muscles and their skeletal supports, try to identify trends in its post-metamorphic development, and comment upon the evolutionary implications of these observations. We anticipate that the new data presented here on this poorly known basal anuran group will be of great utility for future phylogenetic analyses, comparative and functional evaluations, and other studies into anuran biology and evolution.

MATERIAL AND METHODS

***Barbourula* specimens.** Three specimens of *Barbourula busuangensis* were examined (see Table 1). ZRC 1.10828 is a complete fixed ?male specimen from Puerto Princessa, Palawan, Philippines, deposited in the collections of National University of Singapore (NUS). DP FNSP 6554 comprises an articulated skull, disarticulated postcranial skeleton, alizarin-stained hindlimbs, and a hyoid and pectoral girdle stored in formalin; the specimen is in possession of the Department of Paleontology, Charles University, Prague, currently on permanent loan to the Geological Institute of the Academy of Sciences, Prague. The origin of the specimen is unknown, but it is suspected to be from Palawan; it was a gift to the late Prof. Zdeněk V. Špinar of Charles University from the Department of Biology, Silliman University, Dumaguete City, Philippines, during the 1960's. DP FNSP 6582 is a sectioned skull of a fixed female specimen, originally from the collections of the Department of Botany and Zoology, University of Stellenbosch, South Africa, now transferred in the collections of the Department of Paleontology, Charles University, Prague (Fig. 1). The sections are deposited at the repository of the Geological Institute, Academy of Sciences, Prague. The specimen was collected from Palawan, Philippines, but the precise locality is unknown. It was presented to Prof. Cornelius de Villiers of Stellenbosch University by Edward H. Taylor, who collected the Philippine herpetofauna until 1927.

Other material examined. *Alytes obstetricans* (DP FNSP 6457, 6539); *Ascaphus truei* (DP FNSP 6537, 6538, 6550); *Bombina bombina* juv. (DP FNSP 6563); *Bombina variegata* (DP FNSP 6282, 6441, 6590); *Bombina orientalis* (DP FNSP 6557, 6583); *Discoglossus jeanneae* (DP FNSP 6586); *Discoglossus pictus* (DP FNSP 6514, 6570, 6575, 6589; Hubrecht collection of serially sectioned premetamorphic and metamorphic stages); *Discoglossus sardus* (DP FNSP 6571, 6574, 6584); *Liaobatrachus* sp. (CYH 004; DNM D 2166, 2167; GM V2126; IVPP V11525, V12510, V12541, V12717, V13235B, V13236, V13238, V13239 [15], V13245, V13379, V13380, V14068, V14203, V14269, V14270, V14979 [15]; LPM 0030; MV 77).

Age determination. The relative degree of development was inferred from mid-femoral diameter for DP FNSP 6582 and DP FNSP 6554 (Table 1). Although DP FNSP 6582 is adult judging by its external appearance and body size (Table 1, Fig. 1), histological sections show that it is markedly hypo-ossified. This raised the question concerning age of DP FNSP 6582, and whether slightly bigger individual DP FNSP 6554 was older.

We used skeletochronological methods, based on the number and pattern of growth layers formed in bone tis-

TABLE 1. *Barbourula* Specimens Examined

Specimen	Locality	Date collected	Sex	Snout-vent length, mm	Mid-femoral diameter, mm	Approximate age
DP FNSP 6582	Palawan, Philippines	Before 1927	Female	59	1.48	Subadult (skeletally immature)
DP FNSP 6554	?Palawan, Philippines	Before 1970	—	>60	1.82	Adult (skeletally mature)
ZRC 1.10828	Palawan, Philippines	—	?Male	66	—	Adult (skeletally mature)

sue (Castanet and Smirina, 1990), to estimate the age of DP FNSP 6582 and DP FNSP 6554. Annual periodicity in the formation of these layers in Temperate Zone amphibians with a biphasic growth rhythm, when periods of activity alternate with periods of hibernation, is well known and was proven experimentally (Smirina, 1972, 1994; Castanet et al., 1977; Francillon, 1979). Growth layers also occur in tropical and subtropical amphibians (Guarino et al., 1995, 1998; Wake and Castanet, 1995; Esteban et al., 1996; Pancharatna and Deshpande, 2003; Lai et al., 2005; Pancharatna and Kumbar, 2005; Mao et al., 2012). However, annual growth rhythms in amphibians living in regions without sharp seasonal fluctuations of temperature are less pronounced and annual growth layers are indistinct and not easy to recognize. Lines of arrested growth (LAGs), which in Temperate Zone amphibians are used for estimating number of years, often are doubled or multiplied in amphibians living in regions without sharp seasonal fluctuations of temperature, because their formation is influenced by changes of dry and wet seasons (not necessarily corresponding to annual rhythm), seasonal variation in food availability, reproduction, and other periodical exogenous and endogenous factors (Smirina, 1972; Wake and Castanet, 1995; Esteban et al., 1996). *Barbourula busuangensis* is an aquatic frog living in the tropical region, so it is possible that torrential rains plus food deficiency during wet seasons may be the most important factors that determine seasonal rhythms of its growth.

Age of both individuals was determined by examination of transverse cross-sections of the left femur in the middle of the diaphysis at the level of (or close to) the foramen nutricium (Fig. 2*A*, *B*). The bone was decalcified in 5% nitric acid for 16 hours. Sections were cut at 20 μm with a freezing microtome, stained with Ehrlich hematoxylin, and embedded in glycerin (Kleinenberg and Smirina, 1969).

Histological sectioning and 3D reconstruction. DP FNSP 6582 was serially sectioned for histological study and for 3D reconstruction. Because the original method of fixation of the specimen was unknown (it may only be inferred from separation of muscle fibers that it was alcohol based), it was transferred to 4% formalin, then decapitated, and the head was embedded in paraffin, serially sectioned (20 μm), and stained with azan according to Domagk. We basically followed the same method as described in Kleinteich and Haas (2007), the differences were only in used software (see below). All histological sections were digitized using Zeiss Stemi 2000-C microscope with a Nicon Coolpix 950 digital camera mounted on it. Magnification was adjusted according to the largest sections. The images were saved as JPEG files at 2272 × 1704 pixel resolution. A micrometer scale was photographed with the same camera and microscope settings. 3D reconstruction was assembled in modeling and rendering software 3D Studio Max R3.1. As the initial step, we defined the viewport background by selecting the background image with the largest section and with the micrometer scale. The grid was set to 1.0 mm. Then we loaded images of histological sections one after another; the images were loaded in the same scale as viewport background. The first major step was to manually derive contour lines of skeletal structures, muscles, and nerves from the images of all sections, and convert them to NURBS curves. Because all sections were composed of several curves, each curve was given its special number (and color); each set of such curves received a serial number which was identical with that of a real histological section. It was possible to adjust the curves by moving or adding points in higher magnification. Altogether, we produced curves from 893 sections. The second major step was to arrange all these curves in a frontal view (using Front viewport). This alignment was done manually, using combination of distinctive, an-

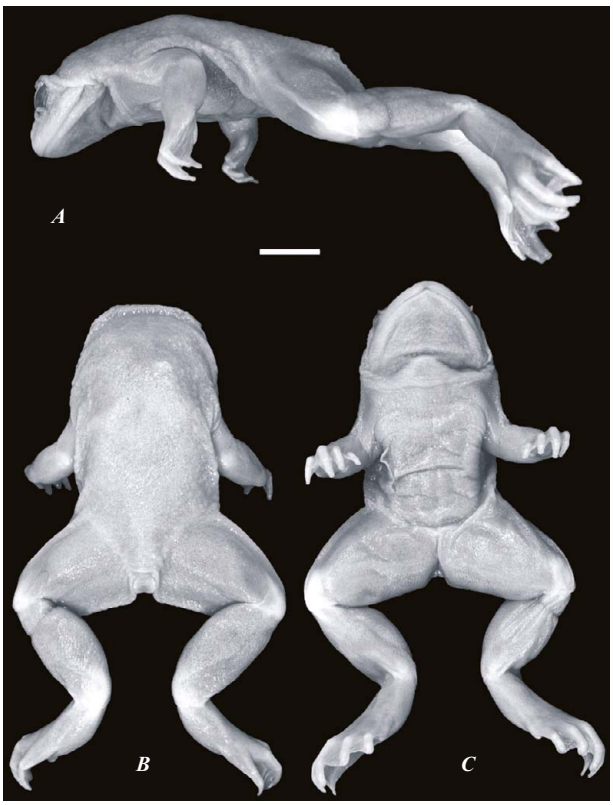

Fig. 1. *Barbourula busuangensis* subadult, not fully grown female (DP FNSP 6582), used for 3D reconstructions based on serial histological sections: lateral (*A*), dorsal (*B*), and ventral (*C*) aspects. Scale bar is 10 mm.

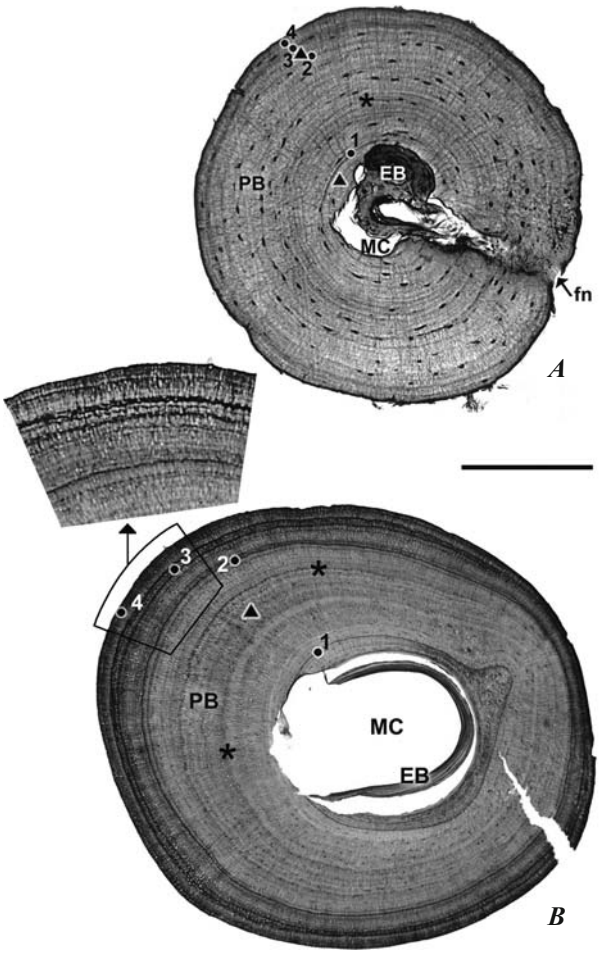

Fig. 2. *Barbourula busuangensis*, haematoxylin stained cross-sections of femur: *A*, subadult, not fully grown female (DP FNSP 6582); *B*, adult, fully developed individual (DP FNSP 6554); PB, periosteal bone tissue; EB, endosteal bone tissue; MC, marrow cavity; fn, foramen nutricium; circles, resting lines or lines of arrested growth (LAGs); triangles, additional lines; asterisk, difficult to determine whether it is LAG or additional line. Scale bar for both sections is 0.5 mm.

tero-posteriorly oriented structures, such as nerves, midpoints of the bottom of the braincase and its dorsal margins, etc., and in series of at least 10 adjacent sections (using Display and Hide tools). Then, as the third major step, we arranged the curves along the longitudinal axis in Side and Top viewports. The distance between subsequent sections in the 3D model was set up according to the grid (1 mm). Because the object was sectioned in 20 μm, we used multiplies of 20 from start point 0.000 (where the first section was positioned); thus, the second section would be 0.02 mm from the first section, the second section 0.04 mm, etc. Because of the total number of serial histological sections (893), we could use 50 sections to represent 1 mm of the skull length, but because size of reconstructed anatomical structures did not require small details, we used only each second section (i.e., 25 sections within 1 mm) for volume rendering. Moreover, in case that a histological section was damaged, we could use adjacent section. All curves of resulting wire 3D model were then extruded, which means that the model received stepped surface. Such output was used for initial, preliminary assessments. For graphic presentation, we created loft surfaces for each sub-object separately from the wire 3D model, using the Force 2-sided rendering option. A necessary prerequisite was that the starting points of all NURBS curves were in the same position (e.g., on the most extreme point of the first curve of a sub-object, and all other curves of the same sub-object had to have their start points in approximately same position). In such case, the curves could be aligned automatically (by Auto Align Curve tool). Minor artifacts in the alignment were rectified by shifting points of curves, which could be still activated. Finally, for presentation purposes the 3D model was rendered to Corel PhotoPaint and if necessary, it could be (but was not necessarily) graphically improved (e.g., when incident light inadvertently emphasized minor irregularities of loft surfaces).

Synchrotron x-ray imaging. Specimen ZRC 1.10828 was fixed in 3.7% formalin, transferred to 75% alcohol and then rehydrated before being placed in an 8-cm polypropylene tube and embedded in Agarose at 3% (without air bubbles), for synchrotron x-ray imaging (Boistel et al., 2011a, 2011b). We used the ID17 long (144 m) imaging beamline of the European Synchrotron Radiation Facility (Boistel et al., 2009; Loetters et al., 2011) with a large field of view and monochromatic beam. The x-ray beam available at ID17 ESRF beamline was produced by a double-Laue monochromator (Suorti et al., 2000). The size of the beam at the sample level was 100 × 3 mm^2 and the energy was tuned to 53 keV to obtain a suitable signal/noise ratio with this kind of sample. The x-ray detector was an in-house FReLoN (Fast Readout Low Noise) camera. It consisted of a 2048 × 2048-pixel CCD-chip cooled to –17 degrees. The pixel size was 15 × 15 $μm^2$. However, to obtain a suitable Field Of View (FOV), the chip was coupled with a tapered bunch of optical fibers to magnify the FOV and the size of the pixel to 80 × 80 mm^2 and 45 × 45 $μm^2$, respectively. The x-ray beam was converted to visible light by means of a Phosphor/Gadolinium screen, 60 μm thick and glued at the surface entrance of the tapered optical fibers. The sample was fixed on a rotating stage located 3 m from the detector. The effective viewing area on the detector is 2048 columns × 50 lines. The detector electronics were set to select only this region to increase the

acquisition speed. Tomographic data were recorded at each vertical slice by rotating the sample in synchronization with the FReLoN acquisition. The acquired sinogram consisted of a 2048 × 3000-pixel angular projection through a 360° sample rotation. One angular projection corresponded to 0.12°. The speed of the rotation was 3°/sec resulting in one angular projection every 40 msec and 120 sec for one slice. The 40 msec are divided in 22 msec effective integration time and 18 msec readout time. To protect the detector from incoming x-rays during the readout time, a fast rotating beam chopper (Renier et al., 2005) was placed upstream from the sample in synchronization with the rotation motor and the FReLoN detector. The final images were reconstructed using dedicated in-house software called HST for "High Speed Tomography" (Chilingaryan et al., 2011). 3D renderings were obtained after semi-automatic segmentation of the volume of interest (VOI) of the skeleton and muscle, using Avizo 7.1 (VSG, Visualization Sciences Group, Merignac, France). After obtaining labels, we converted these into binary images and used them as a mask on the raw data, using the public domain program ImageJ. The direct volume rendering (DVR) technique was applied for the VOI of each bone of the skull. The iso-surface function was used to build a smooth 3D surface from a sub-set of selected voxels of muscles and middle ear structures (cartilage, cavity and bone).

Anatomical nomenclature. Unless otherwise stated, osteological terminology is based on Bolkay (1919), and the nomenclature of the anuran muscles on Luther (1914), with slight modifications (Carroll and Holmes, 1980). Luther developed for the most part the nomenclature of jaw adductors in extant amphibians, which was later modified to some extent. In order to facilitate comparisons with published information on adults of other anurans and caudates, we give an overview of the names used by other authors (Table 2), even for those terms for which partial synonymies have been published (e.g., Edgeworth, 1935; Iordansky, 1996; Johnston, 2011). Synonyms used by earlier authors than Gaupp (1896) are not included here (but see Luther, 1914). Gaupp (1896) is included because it is widely used reference book. One can agree with Haas (2001) that communicating in anatomy is possible only when the same terms are used for the same (i.e., homologous) structures. Thus if we disregard the main deviation from the nomenclature developed by Luther (1914) which, as emphasized by Johnston (2011), was caused by Edgeworth's (1935) differentiating between the terms "adductor" and "levator" (because some authors used other definitions for these two muscle

TABLE 2. Synonymy of Jaw Adductors in Anura and Caudata

Synonymy	Authors, in chronological order
m. adductor mandibulae externus (MAME)	present paper
M. masseter major	Gaupp (1896) (*Rana*)
Extratemporal	Edgeworth (1911) (Anura)
Mandibularis externus	Lubosch (1938) (Anura)
Adductor mandibulae externus	Luther (1914) (Caudata, Anura)
Levator mandibulae externus and levator mandibulae anterior subexternus	Edgeworth (1935) (Caudata, Anura)
M. adductor mandibulae externus	Säve-Söderbergh (1945) (Caudata)
adductor mandibulae externus superficialis	Säve-Söderbergh (1945) (Anura)
musculus levator mandibulae externus	De Jongh (1968) (*Rana*)
Adductor mandibulae externus	Carroll and Holmes (1980) (Caudata) Anura)
Adductor mandibulae externus	Carroll and Holmes (1980) (Anura)
M. adductor mandibulae externus	Iordansky (1992, 1996) (Caudata)
M. adductor mandibulae externus + M. adductor mandibulae lateralis	Iordansky (1992, 1996) (Anura)
m. levator mandibulae externus + portion of m. levator mandibulae externus	Haas (2001) (Caudata)
m. levator mandibulae externus + m. levator mandibulae lateralis	Haas (2001) (Anura)
Adductor mandibulae A2	Diogo (2008); Diogo et al. (2008) (*Ambystoma*)
Adductor mandibulae externus	Johnston (2011) (Anura)
m. adductor mandibulae posterior subexternus (MAMP-subext)	present paper
Adductor mandibulae posterior (Portio subexterna)	Luther (1914) (Caudata)
Adductor mandibulae posterior subexternus	Luther (1914) (Anura)
Adductor mandibulae posterior subexternus	Säve-Söderbergh (1945) (Anura)
Adductor mandibulae posterior subexternus	Carroll and Holmes (1980) (Caudata, Anura)
M. adductor mandibulae posterior	Iordansky (1992) (Caudata)
M. adductor mandibulae articularis	Iordansky (1992) (Anura)

TABLE 2 (continued)

Synonymy	Authors, in chronological order
M. adductor mandibulae posterior seu articularis	Iordansky (1996) (Caudata, Anura)
m. levator mandibulae externus	Haas (2001) (Anura)
m. adductor mandibulae posterior lateralis (MAMP-lat)	present paper
M. masseter minor	Gaupp (1896) (*Rana*)
m. adductor mandibulae posterior lateralis	Luther (1914) (Anura)
Levator mandibulae anterior lateralis	Edgeworth (1935) (Anura)
M. adductor mandibulae posterior lateralis	Säve-Söderbergh (1945) (Anura)
musculus levator mandibulae anterior lateralis	De Jongh (1968) (*Rana*)
Adductor mandibulae posterior lateralis	Carroll and Holmes (1980) (Anura)
Adductor mandibulae lateralis	Iordansky (1996) (Anura)
m. levator mandibulae lateralis	Haas (2001) (Anura)
Adductor mandibulae lateralis	Johnston (2011) (Anura)
m. adductor mandibulae posterior articularis (MAMP-art)	present paper
Adductor mandibulae posterior articularis	Luther (1914) (Anura)
Adductor mandibulae posterior (P. articularis)	Luther (1914) (Caudata)
Levator mandibulae anterior articularis	Edgeworth (1935) (Anura)
M. adductor mandibulae posterior articularis	Säve-Söderbergh (1945) (Anura)
M. temporalis internus	Stephenson (1951) (*Leiopelma*)
musculus levator mandibulae anterior articularis	De Jongh (1968) (*Rana*)
Adductor mandibulae posterior articularis	Carroll and Holmes (1980) (Caudata, Anura)
Adductor mandibulae posterior	Iordansky (1996) (Anura)
m. levator mandibulae articularis	Haas (2001) (Anura)
Adductor mandibulae posterior	Johnston (2011) (Anura)
m. adductor mandibulae posterior longus (MAMP-long)	present paper
M. temporalis	Gaupp (1896) (*Rana*)
Adductor mandibulae posterior longus	Luther (1914) (Anura)
Adductor mandibulae posterior (P. longa)	Luther (1914) (Caudata)
Levator mandibulae posterior	Edgeworth (1935) (Anura)
M. adductor mandibulae posterior longus	Säve-Söderbergh (1945) (Anura)
musculus levator mandibulae posterior	De Jongh (1968) (*Rana*)
Adductor mandibulae posterior longus (temporalis)	Carroll and Holmes (1980) (Caudata, Anura)
m. levator mandibulae longus	Haas (2001) (Anura)
Adductor mandibulae longus	Johnston (2011) (*Leiopelma*, *Ascaphus*)
m. adductor mandibulae internus (MAMI) divided into **main**, **middle** and **posterior** parts	present paper
M. pterygoideus	Gaupp (1896) (*Rana*)
Pterygoideus	Edgeworth (1911) (Caudata)
M. pterygoideus	Luther (1914) (Caudata, Anura)
Pterygoideus anterior	Lubosch (1938) (Anura)
Levator mandibulae anterior	Edgeworth (1935) (Caudata, Anura)
M. pseudotemporalis superficialis + M. pseudotemporalis profundus	Säve-Söderbergh (1945) (Anura)
musculus levator mandibulae anterior	De Jongh (1968) (*Rana*)
M. temporalis externus (only MAMI-middle part)	Stephenson (1951) (*Leiopelma*)
Adductor mandibulae internus — divided into pterygoideus and pseudotemporalis (further subdivided into a superficialis and profundus head) portions	Carroll and Holmes (1980) (Caudata)
Adductor mandibulae internus	Carroll and Holmes (1980) (Anura)
M. pseudotemporalis anterior (seu profundus) + + M. pseudotemporalis posterior (seu superficialis)	Iordansky (1992) (Caudata)
M. pseudotemporalis (= M. pseudotemporalis anterior of Caudata)	Iordansky (1992, 1996) (Anura)
m. levator mandibulae internus	Haas (2001) (Caudata)
Adductor mandibulae A3" + Adductor mandibulae A3'	Diogo (2008); Diogo et al. (2008) (*Ambystoma*)
Adductor mandibulae internus (rostralis, caudalis)	Johnston (2011) (*Leiopelma*, *Ascaphus*)

Note. Synonyms used by authors earlier than Gaupp (1896) are not included (but see Luther, 1914). Gaupp (1896) is included because it is widely used reference book.

categories, and because the term "jaw adductors" became widely used), the problem is shifted to criteria of homology. It is generally agreed that the most reliable criterion is innervation of muscles, because the nervous system, in terms of its morphological adaptations, is one of the most conservative organ systems of vertebrates. But for jaw adductors this criterion is too general. Topographic relations to branches of the trigeminal nerve as a principal criterion of identity of jaw adductors was criticized by Iordansky (1992, 1996), and Haas (2001) and his collaborators. Here we use it for practical reasons, as a complement to anatomical description, but we take the origins and insertions of muscles as the main criteria of homology, although we admit that the location and extent of muscle origins and insertions may change due to changes in muscle function.

We use the term 'angulare,' which was introduced by Cuvier (1824: 89 – 90), rather than 'angulospleniale,' because the splenials were already lost in late Paleozoic temnospondyls. With the exception of *Xenopus* (Bernasconi, 1951), the dermal part of the anuran lower jaw takes its origin from only two ossification centers, those of the dentale and angulare. Compare the situation in urodeles, in which the goniale (= prearticulare) is preserved (Duellman and Trueb, 1986; Lebedkina, 2004).

Anatomical abbreviations. CN1, nervus olfactorius; CN2, nervus opticus; CN3, nervus oculomotorius; CN4, nervus trochlearis; CN6, nervus abducens; CN10, nervus vagus; LAG, layer of arrested growth; LC, length of skull; LtC, width of skull; MAME, m. adductor mandibulae externus; MAMI, m. adductor mandibulae internus; MAMP-art, m. adductor mandibulae posterior articularis; MAMP-lat, m. adductor mandibulae posterior lateralis; MAMP-long, m. adductor mandibulae posterior longus; MAMP-subext, m. adductor mandibulae posterior subexternus; MLB, m. levator bulbi; MO-inf, m. obliquus inferior; MO-sup, m. obliquus superior; MR-ext, m. rectus externus; MR-inf, m. rectus inferior; MR-int, m. rectus internus; MR-sup, m. rectus superior; MRB, m. retractor bulbi.

Institutional abbreviations. CYH, Chaoyang Bird Fossil National Geopark, Chaoyang, Liaoning, China; DNM D, Dalian Natural Museum, Dalian, Liaoning, China; DP FNSP Department of Palaeontology, Faculty of Natural Sciences, Charles University, Prague, Czech Republic; GM, Geological Museum of China, Beijing, China; IVPP, Institute of Vertebrate Paleontology and Paleoanthropology, Beijing, China; LPM, Liaoning Paleontology Museum, Shenyang, Liaoning, China; MV, Nanjing Institute of Geology and Paleontology, Chinese Academy of Sciences, Nanjing, Jiangsu, China; ZRC, National University of Singapore, Singapore.

RESULTS

Age of the *Barbourula* Specimens

We interpret the dark LAGs (Fig. 2*B*) as annual growth rings, with some additional lines present in the larger individual, DP FNSP 6554. Our interpretation is based on the observation that both DP FNSP 6582 and DP FNSP 6554 have the same pattern of growth layers, despite they were collected independently, at different times. Thus, it seems unlikely that the same pattern of LAGs be induced by occasional climatic events.

The LAGs interpreted as corresponding to the first to second year of life of DP FNSP 6582 and DP FNSP 6554 are indistinct, with numerous additional, false lines (Fig. 2*A*, *B*). The large distance between the first and second LAG indicates rapid growth. After the second year, annual layers abruptly became narrow, which indicates attaining sexual maturity and arrest of growth. The outermost, fourth LAG is close to the surface of the bone.

We cannot be fully certain that the number of LAGs observed in DP FNSP 6582 and DP FNSP 6554 accurately reflects age, because one-year-old individuals, which in other species indicate rate of early endosteal resorption (Leclair and Castanet, 1987; Smirina and Makarov, 1987; Castanet and Smirina, 1990), were not available. Resorption of innermost one or more LAGs, corresponding to the first years of life, reduces actual age of the animal by one or more years. Nevertheless, we can estimate from the number of distinguishable LAGs that both individuals are not younger than four years. Based on these considerations, we consider 4 – 5 years for DP FNSP 6582 and 4 – 6 years for DP FNSP 6554 a reasonable estimate of age.

ZRC 1.10828 could not be examined skeletochronologically. It is an adult of relatively large size (Table 1).

Anatomical Description

Exocranium. We focus our description of the exocranium of *Barbourula busuangensis* on features not described in the previous accounts by Trueb (1973) or Clarke (1987, 2007), with the exception of features for which our observations disagree with these earlier accounts, and features that change during postmetamorphic development.

The facial process of the premaxilla is vertical and short, and well separated from the nasal. The maxilla lacks a zygomatico-maxillar process (Fig. 4*C*, *O*) and lacks contact with the squamosal (Fig. 4*C*, *D*). Its anterior part is deep, terminated by two or three processes (Clarke, 2007). Only the ventral process abuts the premaxilla, whereas the dorsal process terminates freely

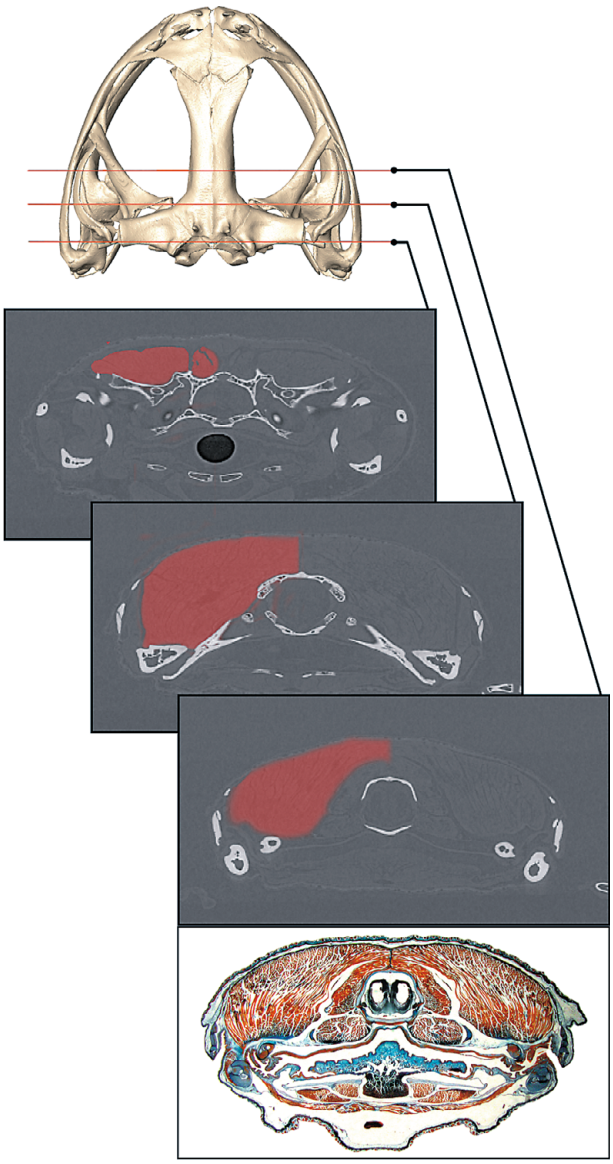

Fig. 3. Dorsal view of skull of *Barbourula* (ZRC 1. 10828) with three tomograms taken at the levels indicated by cross-lines, to show distinction of bones and muscles on tomograms. MAMP-long on the left side of tomograms highlighted in red. A photograph of a histological section of the specimen DP FNSP 6582 corresponding to the lowermost tomogram is shown for comparison. Note orientation of muscle fibers, separated from each other after alcohol based fixation.

(marked by arrow in Fig. 4*C*). The frontal process is pointed, abutting against the lateral process of the nasal (Fig. 4*D*, *O*). The pterygoid process is moderately extended. Posteriorly, the maxilla has an extensive contact with the quadratojugal (Fig. 4*D*). In subadult female DP FNSP 6582 the quadratojugal is not fused to the quadrate, which is still cartilaginous, but it is coalesced to the quadrate in fully grown adults. A calcified sesamoid is present in ZRC 1.10828 (Fig. 4*F*).

The medial margins of the nasals are long and straight; only their posterior sections are divergent. The nasals are bordered anteriorly by a rhomboid field between the nasals and frontoparietals, where the dorsal surface of the sphenethmoid is exposed (Fig. 4*B*). In the subadult female, the nasals are still small, covering only part of the nasal capsules (Fig. 5*H*). In the fully grown adult specimens, the antero-lateral margin of each nasal bears a pointed parachoanal process (Fig. 4*B*, *D*, *F*, *J*), directed towards the dorsal process of the anterior end of the maxilla (Fig. 4*D*). Laterally, the nasal consists of two layers that enclose the dorso-medial part of the lateral diverticulum of the nasal organ (Fig. 4*J*; see also Jurgens, 1971). Serial sections show that in the subadult female, this region was preformed by two parallel tissue layers. The frontoparietals are fused in the midline, and the line of coalescence is marked by a low median ridge (Fig. 4*B*, *C*). In the subadult female, the frontal portions of the frontoparietals are separated by a narrow fontanelle, extending over the anterior part of the frontoparietal fenestra of the sphenethmoid. Remnants of the fontanelle may be preserved in adults (Fig. 4*D*). The anterior tips of the frontoparietals are widely divergent (Fig. 4*B*, *L*, *M*). The middle portion of the frontoparietals has ventrally deflected margins, which give the bone a semi-tubular shape. The parietal portion of the frontoparietal produces a pair of prominent spike-like processes (Fig. 4*B*, *D*, *L*). Incrassations on the inner surface of the frontoparietal, which fit into the fenestrae in the roof of the braincase, consist of an anterior and a posterior part (Fig. 4*M*). The posterior part of the alar lamella of the squamosal is strongly reduced whereas its anterior portion is long, but not in contact with the maxilla (Figs. 4*C*, *D*). The ramus paroticus is poorly developed (Fig. 4*D*) and connected to the crista parotica of the otic capsule by soft tissue.

The vomer has a well-developed anterior portion, which approaches the horizontal lamina of the premaxilla, but the vomer and premaxilla do not contact each other. Because the anterior portion of the vomer borders the choanal opening anteriorly, the posterior part of the vomer may be considered a homolog of the anterior choanal process. The posterior choanal process, which borders the choana posteriorly, is slender and short. A free palatine is absent. The cultriform process of the parasphenoid is relatively broad in its posterior third, at which point it bears prominent ridges along its margins. These ridges diverge onto each lateral ala, where they delimit a sloping surface to which the retractor bulbi muscle (MRB) is attached. The lateral margins of the cultriform process taper abruptly in the middle of the prootic fonta-

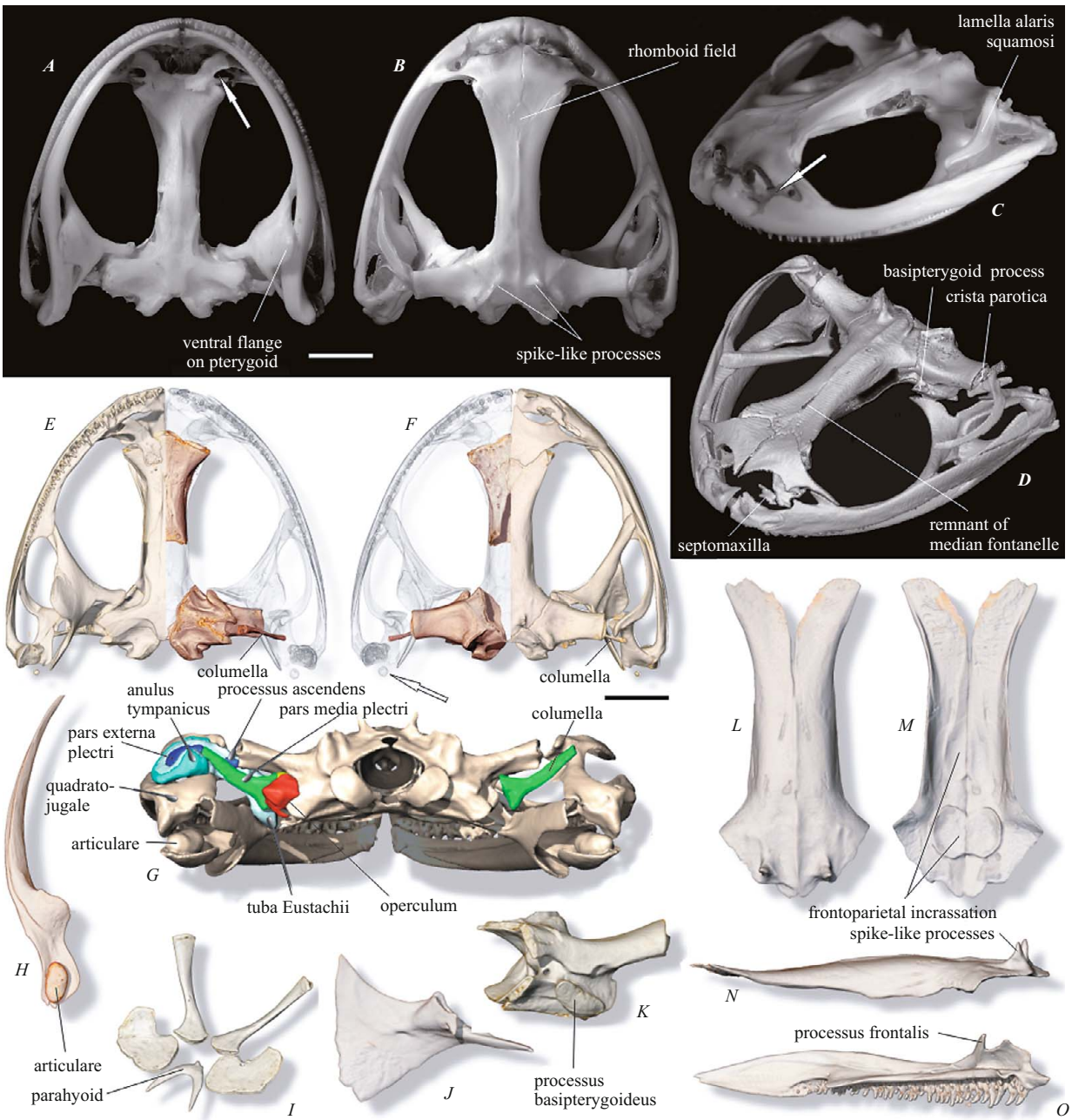

Fig. 4. *Barbourula busuangensis*. Exocranium of DP FNSP 6554 in ventral (*A*), dorsal (*B*), and in left dorsal and slightly anterior (*C*) aspect; *D* – *O*, ZRC 1.10828, synchrotron x-ray images. Cartilaginous parts not illustrated; *D*, in same aspect as *C*; in ventral (*E*) andin dorsal (*F*) aspects, with dermal bones of left half illustrated for topographic orientation as if transparent, to show endocranial ossifications (sphenethmoid, prootico-occipital, columella); *G*, skull in posterior aspect, to demonstrate topographic relationships of middle-ear components; *H*, left angular in dorsal aspect, with ossified articular; *I*, ossifications of the hyoid (hyoid in the same aspect as in *C* and *D*); *J*, left nasal in dorsal view, to show thickened lateral portion with two layers that enclose the dorso-medial part of the diverticulum laterale of the nasal organ; *K*, left prootico-occipital in anterior aspect, to show basipterygoid process; *L* – *N*, frontoparietals in dorsal (*L*), ventral (*M*), and left lateral (*N*) views. Note frontoparietal incrassations in *M*; *O*, left maxilla in lingual aspect. Arrow in (*A*) marks position of choana, arrow in (*C*) marks dorsal process of anterior part of maxilla, arrow in (*F*) points to sesamoid bone. Scale bars in (*A*, *B*) and (*E*, *F*) are 5 mm.

nelle, and where the cultriform process adjoins the posterior part of the sphenethmoid; thus the anterior third of the process tapers to a thin point. The maxillary ramus of the pterygoid (Fig. 4*B*, *D*, *F*) abuts not only the ptery-

goid process of the maxilla along its entire dorsal surface, but also leans against the medial surface of the vertical part of the maxilla. Similarly, the interior ramus is attached perpendicularly to the basipterygoid process of the prootic. The ventral flange (sensu Trueb, 1973) is prominent, and its lateral surface serves as a guide for the lower jaw (Fig. 4*A*).

The angulare (angulospleniale of some authors; see *Anatomical Nomenclature* section) bears an extensive coronoid process (Fig. 4*H*). The V-shaped parahyoid bone had not yet developed in the subadult female specimen, but was present in ZRC 1.10828 (Fig. 4*I*).

Endocranium. The serially sectioned subadult female endocranium confirms many of the details of the anatomy and innervation of the ethmoidal region of *Barbourula busuangensis* described by Jurgens (1971), including the origin of the inferior prenasal cartilage from the solum nasi, the large fenestra nasobasalis, and the narrow anterior part of the tectum nasi (Figs. 5*A*, 6*A*). The nasal cavity extends far posteriorly along the anterior portion of the braincase, and the posterior parts of both nasal capsules are widely separated by the braincase, as in *Ascaphus*, *Leiopelma*, and *Bombina* (Pusey, 1943; Jurgens, 1971). The lateral portion of the inferior diverticle extends into the mouth cavity (Fig. 5*F*, *G*, *H*); the medial portion, termed the diverticulum mediale or Jacobson's organ by Jarvik (1942), is restricted to the prechoanal part of the nasal sac. However, the medial portion of the inferior diverticle is markedly exceeded by the principal diverticle, which extends into the most posterior part of the nasal cavity, as far as the level of the anterior half of the orbit. At the level of the postnasal wall (Fig. 5*G*), both nasal capsules are separated from one another by only a thin nasal septum, which terminates at the level of the anterior part of the eye. As a result, both olfactory canals are very short and the olfactory tracts run unseparated in the braincase. Another characteristic feature of *Barbourula* is that the anterior portion of the lateral diverticle of the olfactory sac turns, as an accessory sac, dorsally over the lateral surface of the oblique cartilage (Fig. 5*E*; Jurgens, 1971). The preformation of the anterior portion of the nasal in the subadult female specimen and the isolated nasals of the adult *Barbourula* specimens (Fig. 4*J*) confirm that the accessory sac inserts between two layers of the lateral part of the nasal, which form a deep longitudinal trough, as noted by Jurgens (1971).

The sphenethmoid and the orbital part of the braincase are tube-like (Figs. 4*E*, *F* and 6*A*). Based on comparison between the subadult and adult specimens, ossification of the sphenethmoid begins posteriorly and spreads anteriorly and laterally into the postnasal walls. The lateral wall of the ossified part is pierced by a canal (Figs. 5*I* and 6*A*) for the ramus medialis n. ophthalmici, and the roof opens via a long frontal fenestra, which is separated from the parietal fenestra by the tectum transversum (Fig. 6*A*). In articulated skulls, the fenestrae are filled with the frontoparietal incrassations (Fig. 4*M*). The prootic fontanelle (Fig. 6*A*) is divided by a horizontal partition in the dorsal and ventral portions. Cranial nerve (CN) 5, CN6, and CN7 pass through the dorsal portion. A similar division of the prootic fontanelle can be seen in *Ascaphus*, but unlike *Barbourula*, *Ascaphus* has a separate foramen for CN7 (de Villiers, 1934).

The crista parotica of the otic capsule is adjoined anteriorly by the otic process of the palatoquadrate (Fig. 7*B*). The otic process of the palatoquadrate is cartilaginous even in fully grown adults, whose otic capsules are completely ossified. In our sectioned subadult female, the crista is histologically distinguishable from the cartilaginous capsule, and preserves its identity as a derivative of the palatoquadrate.

The palatoquadrate is a vertical plate, the dorsal margin of which is deflected laterally to form a horizontal lamina that supports the Eustachian tube ventrally (Figs. 6*A* and 7*B*). Posteriorly, the vertical part decreases in depth and only the horizontal lamina continues to the jaw joint (Fig. 7*E*, *F*). In our subadult female, a thin subocular bar (the larval commissura quadrato-cranialis anterior) is fused to the lateral end of the postnasal wall, which is a typical condition for adults (Fig. 6*A*). This contrasts with the otic and basal articulations of the palatoquadrate, which are still separated from the otic capsule (Figs. 7*A*, *B* and 8*I*). The basal articulation (Figs. 4*D*, 7*A*, *B*, and 8*I*) consists of separate basal and basipterygoid processes, even in mature adults; the basipterygoid process is ossified and manifested as a prominent outgrowth on the anterior surface of the prootic (Fig. 4*K*), surrounded by the flared tip of the medial ramus of the pterygoid.

The quadrate and articular are cartilaginous in the subadult female specimen, but calcified and fused to the quadratojugal and angular (Fig. 4*H*), respectively, in fully grown individuals. Sesamoids were regularly found in adults (Fig. 4*F*; see also Clarke, 1987). The mentomeckelian element is ossified and fused to the dentale.

The middle ear apparatus is complete (Figs. 4*G* and 6*B*). The columella consists of extended and moderately bifurcated pars interna plectri, a slender, ossified shaft termed pars media plectri, and the pars externa embedded in the tympanic membrane (Fig. 6*A*, *D*). The membrane is stretched within the anulus tympanicus, which is an almost complete cartilaginous cup-like structure interrupted only on its dorsal side. The pars externa seems to have a movable joint with the pars media, and is con-

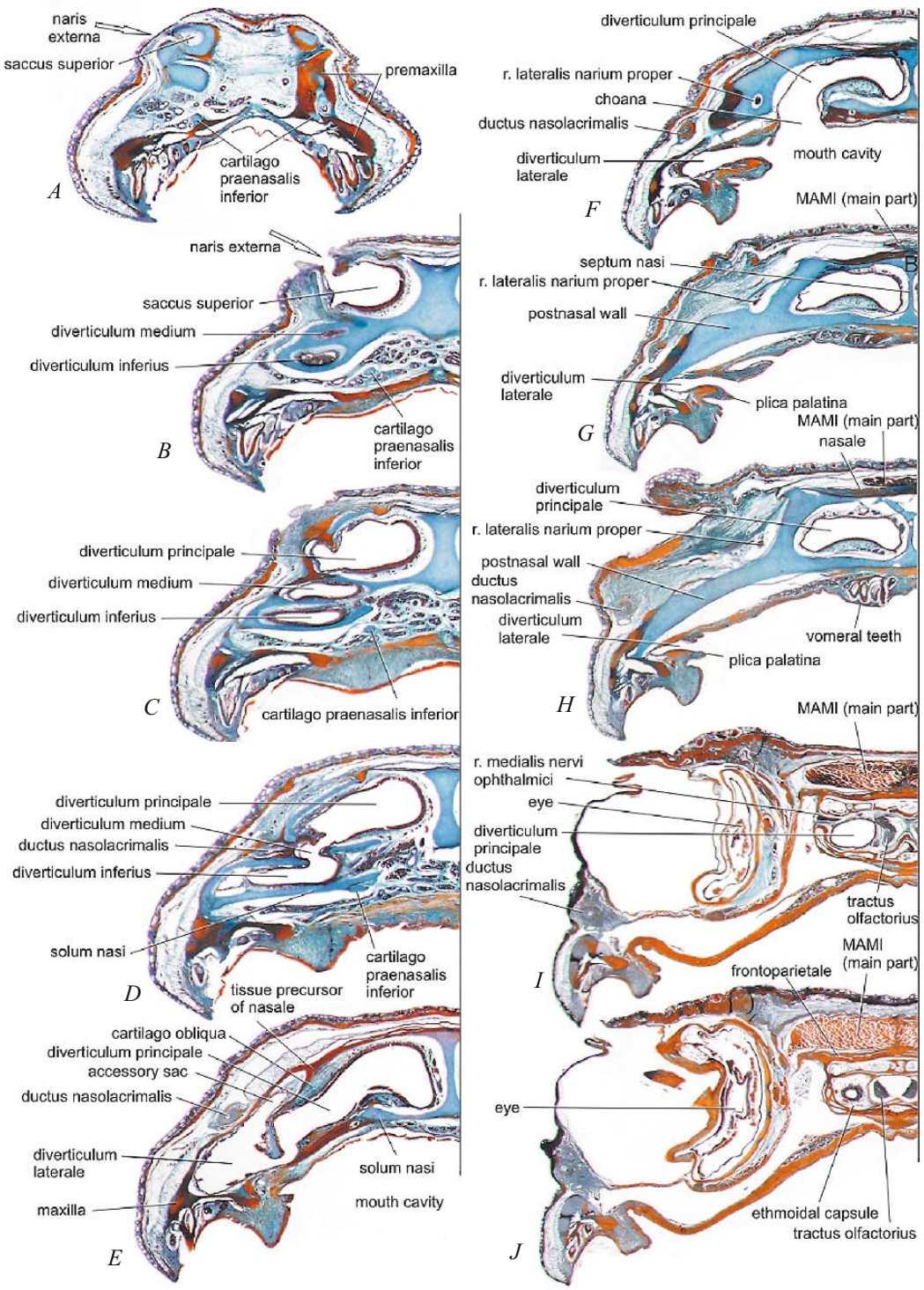

Fig. 5. Transverse sections through the nasal region of *Barbourula busuangensis* (DP FNSP 6582): *A*, anterior part of the head at the level of facial process of premaxilla; *B*, section at the level of external naris; *C*, subdivision of anterior part of nasal capsule; *D*, origin of ductus nasolacrimalis; *E*, antero-lateral, double-layered portion of nasal (here still represented by connective tissue) with dorsal extension of diverticulum laterale (accessory sac); *F*, choana, posterior part of recessus lateralis, and anterior orifice of the canal for the ramus lateralis narium proper; *G*, anterior end of main part of MAMI; *H*, attachment of commissura quadrato-cranialis anterior to the neurocranium; *I*, origin of the olfactorius tract within the most anterior part of braincase; *J*, overlapping of the nasal capsules and braincase posterior to the postnasal wall. Sections not to scale. Only left halves of sections are illustrated in (*B* – *J*).

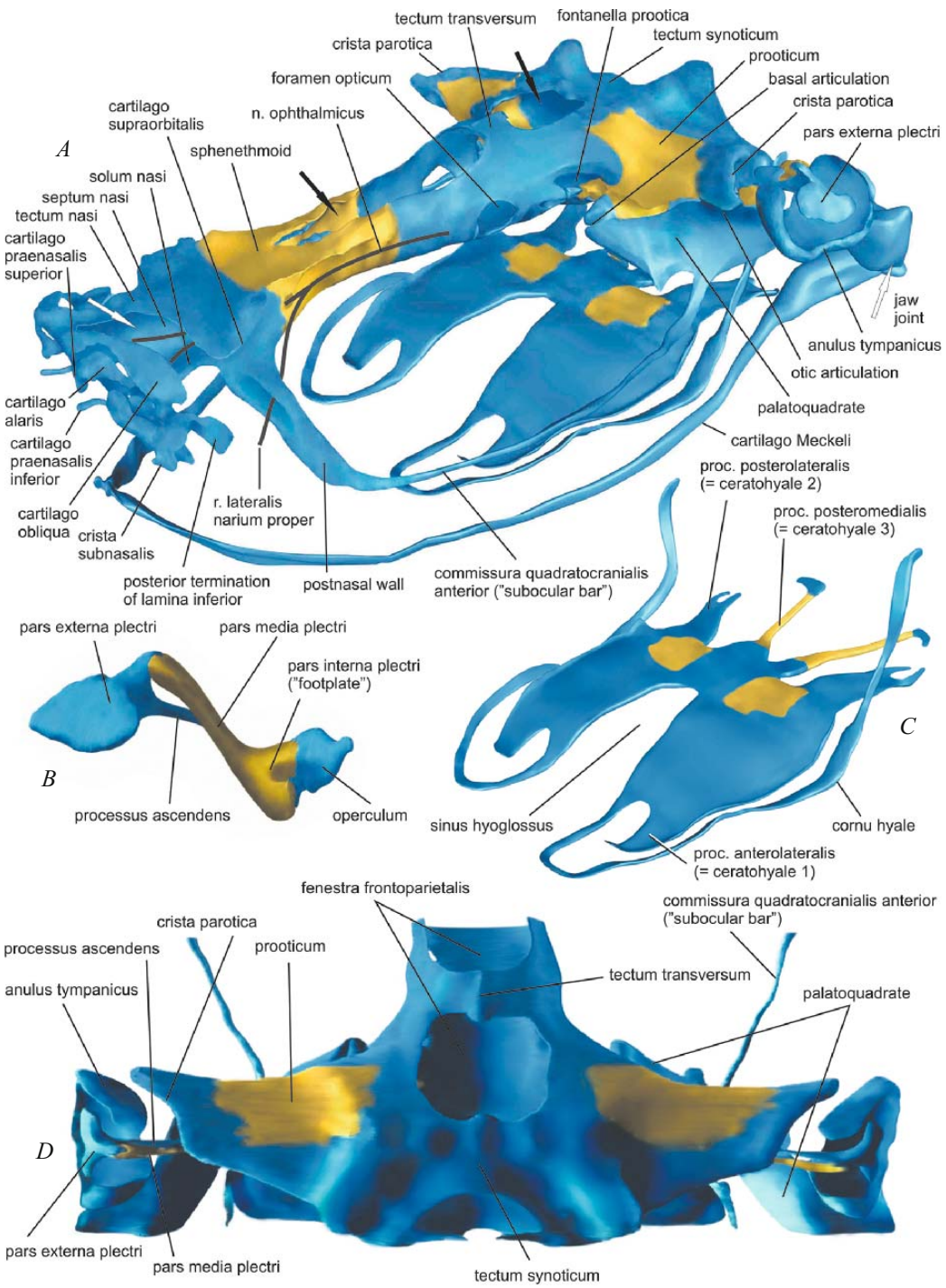

Fig. 6. Three-dimensional reconstruction of endocranium of *Barbourula busuangensis* (DP FNSP 6582): *A*, anterolateral and slightly dorsal aspect. White arrow marks fenestra nasolateralis, black arrows mark frontoparietal fenestra divided by tectum transversum; *B*, left plectral complex with some associated structures in posterolateral aspect; *C*, hyoid (same view as in *A*); *D*, otic region of skull in dorsal aspect. Cartilage blue, endochondral bone yellow. Only (*A*) and (*C*) are at the same scale.

nected to the lower surface of the crista parotica by a thin processus ascendens.

The hyoid (Figs. 4*I* and 6*C*) has two endochondral ossifications within the main body, which belong to the

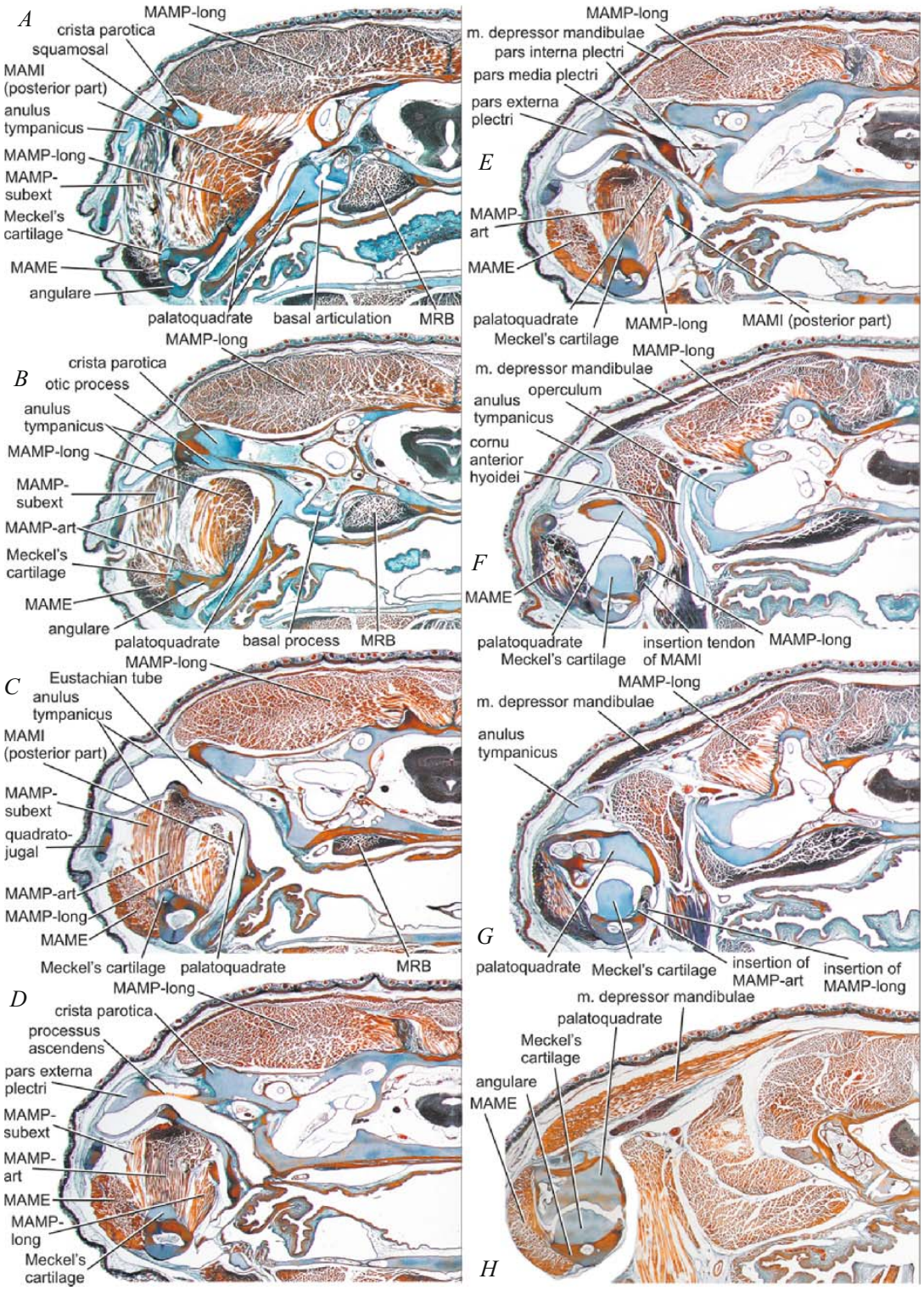

Fig. 7. Transverse sections through the otic region of *Barbourula busuangensis* (DP FNSP 6582): *A*, anterior end of otic capsule and basal articulation; *B*, processus oticus palatoquadrati. Note its fusion to crista parotica; *C*, Eustachian tube and series of adductors below it. Note posterior part of MAMI and MAMP-long; *D*, processus ascendens of pars externa plectra; *E*, middle ear structures and posterior attachments of jaw adductors; *F*, relations between cornu anterior hyoidei and operculum; *G*, section anterior to jaw joint; *H*, jaw joint (note it consists still of cartilage), posterior part of MAME, and depressor mandibulae. Only left parts of sections are illustrated.

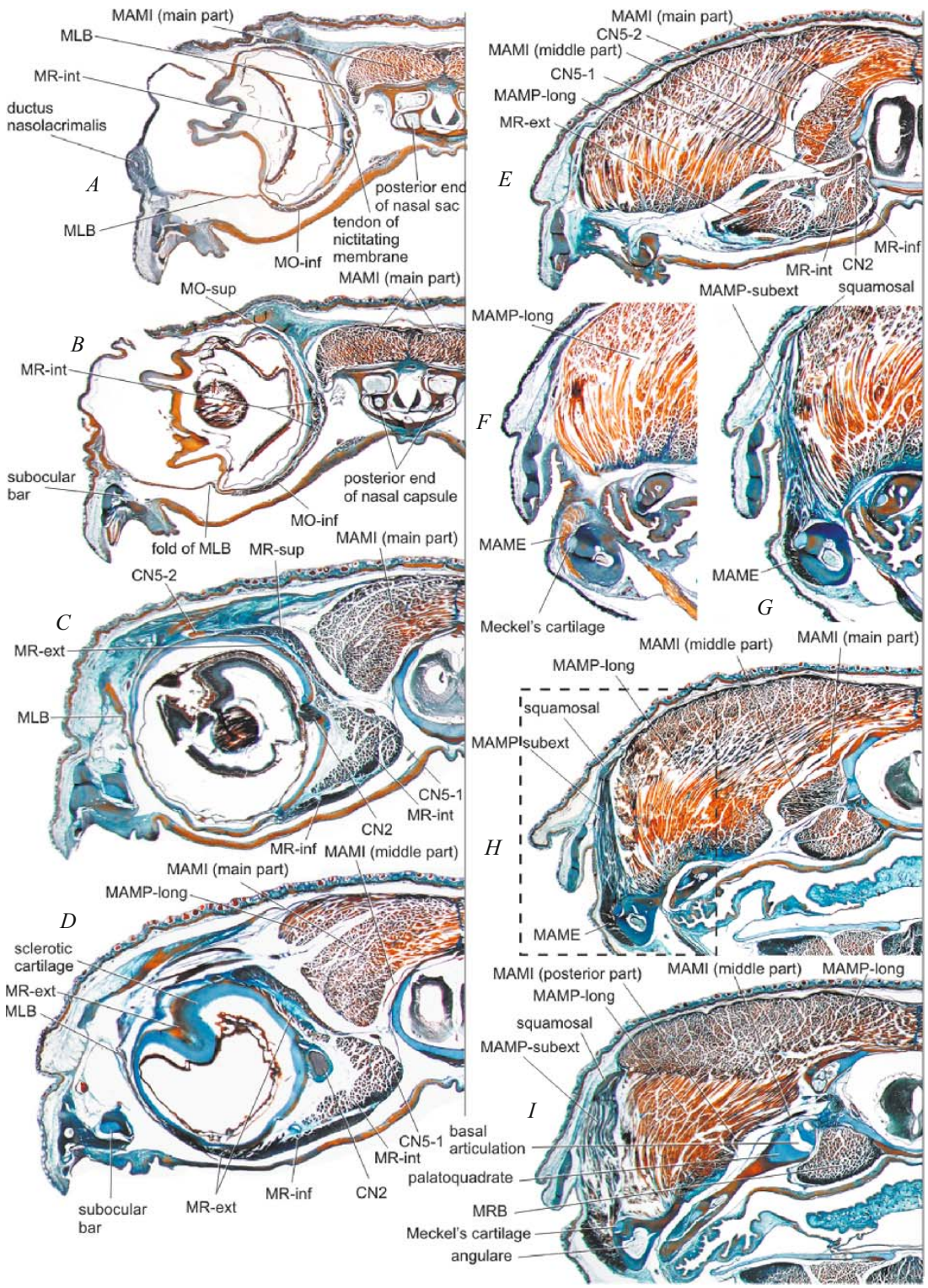

Fig. 8. Transverse sections through the orbital region of *Barbourula busuangensis* (DP FNSP 6582): *A*, anterior part of braincase; *B*, posterior termination of nasal capsules; *C*, anterior end of MAMP-long; *D*, anterior end of middle part of MAMI; *E*, passage of the optic nerve through braincase wall; *F*, anterior end of MAME; *G*, connection of MAME with MAMP-long by means of MAMP-subext; *H*, posterior termination of main part of MAMI, and its connection with middle part of MAMI. Broken line marks area illustrated in (*F*) and (G); *I*, connection between middle and posterior parts of MAMI. Only left halves of sections are illustrated in (*A* – *E*) and (*H* – *I*).

posterolateral processes. The ossified posteromedial processes extend beyond the main body of the hyoid.

Cranial nerves. In *Barbourula busuangensis*, CN5 splits into three branches, CN5-1 (n. ophthalmicus), CN5-2 (ramus maxillaris), and CN5-3 (ramus mandibularis), similar to other anurans. CN5-1 leaves the braincase through the dorsal portion of the prootic fontanelle and runs between the middle portion of the adductor mandibulae internus muscle (MAMI) and the dorsal surface of the MRB anteriorly (Fig. 8*E*). CN5-2 and CN5-3 leave the trigeminal ganglion by a common stem, which passes through the dorsal portion of the prootic fontanelle and runs anteriorly between MAMI and the adductor mandibulae posterior longus muscle (MAMP-long). The two rami split from one another above the posterior part of the eye-ball; CN5-2 terminates above the lateral part of the eye-ball, whereas CN5-3 runs along the lateral surface of MAMP-long posteriorly, where it passes between the posterior part of the adductor mandibulae posterior subexternus muscle (MAMP-subext) and the adductor mandibulae externus muscle (MAME). Iordansky (1992) and Haas (2001) reported that the position of CN5-3 varies among anuran genera and passes laterally to the MAME in some taxa (e.g., *Bombina*, *Discoglossus*). Variation in the course of CN5-3 is most probably a result of posterior rotation of the palatoquadrate below the otic capsule during metamorphosis (Iordansky, 1992).

CN7 originates from the medulla oblongata and closely adjoins CN8 (n. statoacusticus) ventrally (n. acusticofacialis of de Villiers, 1934). After separating from one another, CN7 passes anteriorly, enters the medial wall of the otic capsule, and runs within the wall of the braincase to the posterior end of the trigeminal ganglion, where it returns to the braincase cavity. However, it does not merge with the ganglion. Instead, it turns laterally into the dorsal portion of the prootic fontanelle. It should be noted that in *Ascaphus*, CN8 runs through a separate facial foramen posterior to the ventral portion of the prootic fontanelle (de Villiers, 1934). There it receives a sensory branch, the ramus palatinus, which comes from the mucous membrane of the mouth palate. From this point, the main stem is termed the ramus hyomandibularis. It turns around the basal articulation posteriorly and crosses the Eustachian tube dorsally. Posterior to the columella, it splits into three branches; one of them meets the ramus communicans of CN9, thus constituting Jacobson's anastomosis (Schlosser and Roth, 1995). Thus the characteristic feature of CN7 of *Barbourula* is that it does not enter the trigeminal ganglion, nor does it have any connection between the trigeminal ganglion and the ramus palatinus of CN7 by means of a commissural nerve, as in *Ascaphus*.

Adductors of the lower jaw. As mentioned above (see the section Anatomical Nomenclature), homologies of lower jaw adductors have been inferred among terrestrial tetrapods from topographic relations to principal branches of CN5 (Luther, 1914; Säve-Söderbergh, 1936; Carroll and Holmes, 1980). For practical reasons, we maintain notes on relations of these muscles to CN5 in our descriptions, but consider muscle origins and insertions as other relevant and significant criteria for decisions on muscle homology. See also Table 2 for synonyms used in papers of other authors. Muscles in the posterior part of the orbit, which run between CN5-1 and CN5-2, are called collectively the adductor mandibulae internus (MAMI). Those that lie between the common stem of CN5-2 and CN5-3, and the distal, posteriorly running CN5-3, are called the adductor mandibulae posterior (MAMP). Those that are lateral to the distal, posteriorly running CN5-3 are called adductor mandibulae externus (MAME; but see the note on variation of CN5-3 above).

The MAME of *Barbourula busuangensis* is strongly reduced compared, e.g., with *Rana*. It has an antero-posteriorly extensive insertion on the lateral surface of the lower jaw (Figs. 9*A* and 10*A*), but is only attached to the upper jaw close to the jaw joint. Further anteriorly, it is either attached by means of the MAMP-subext to MAMP-long (Figs. 9*A* and 10*B*), or, close to its anterior end, it terminates freely just behind the mouth corner (Fig. 8*F*). Posteriorly, it is well separated from the depressor mandibulae; the latter muscle originates at the posterior end of the articulare (if ossified); if the posterior end of the articulare is still cartilaginous, as is the case in the subadult female (DP FNSP 6582), then the entire depressor mandibulae originates from the angulare and outer surface of MAME, similar to the most posterior part of the MAME in the adult condition. The MAME decreases in size anteriorly, and its insertion is shifted onto the lateral surface of the angulare. Two parts of MAME can be distinguished. In its posterior portion, the lower, outer part consists of horizontal fibers, whereas the upper, inner part consists of vertical fibers attached to the lateral surface of Meckel's cartilage. Anterior to the jaw joint and below the anulus tympanicus, the conditions are reversed — the outer layer of MAME consists of vertical fibers stretched between the quadratojugal and outer surface of the angular, and the inner layer consists mainly of horizontal fibers.

MAMP is subdivided into four easily recognizable portions that were considered separate anuran muscles by Luther (1914): the subexternus portion (MAMP-subext), which usually originates on the medial surface of the lamella alaris of the squamosal, the lateralis portion (MAMP-lat), which originates on the medial surface of

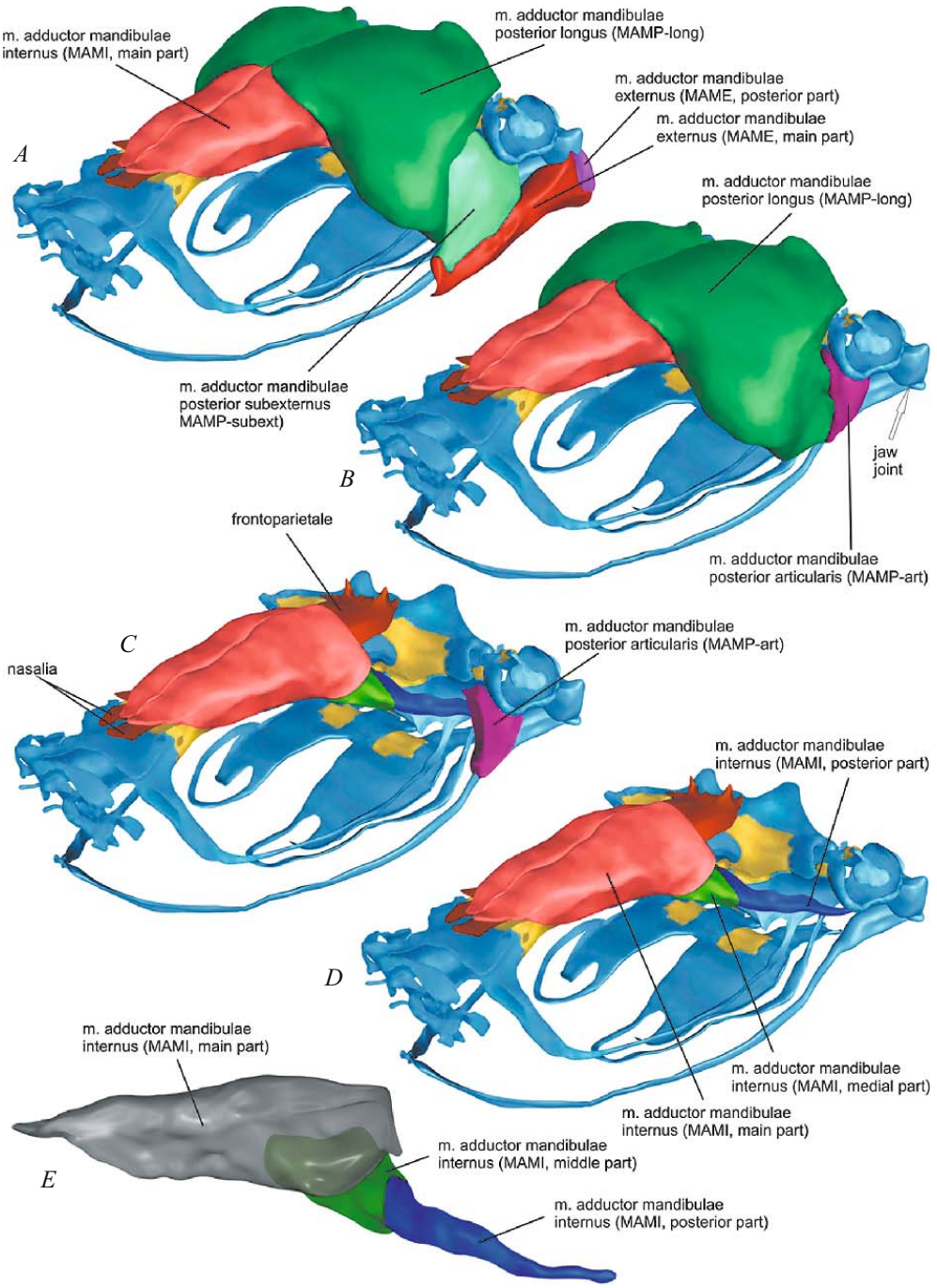

Fig. 9. Three-dimensional reconstructions of jaw adductors of not fully grown *Barbourula busuangensis* (DP FNSP 6582) and their topographic relationships with endocranium, nasals and frontoparietals: *A*, complete system of jaw adductors; *B*, same as in (*A*), but MAMP-subext and MAME removed; *C*, same as in (*B*), but MAMP-long removed; *D*, same as in (*C*), but MAMP-art removed, to show composition and extent of MAMI; *E*, MAMI in lateral view. The main part of MAMI is transparent to show its relationship with the middle part of MAMI; *A* – *D*, in the same aspect as in Fig. 6*A*, *D*, in left lateral aspect. Dermal bones (frontoparietals and nasals) brown, color code of endoskeletal structures same as in Fig. 6.

the posterior part of the lamella alaris squamosi and quadratojugal, the articularis portion (MAMP-art), originating from the ventral surface of the palatoquadrate, and the longus portion (MAMP-long), which is the strongest of all adductors (Figs. *7* and 9*A*, *B*). It originates from the parietal and adjacent parts of the otic capsule, and runs

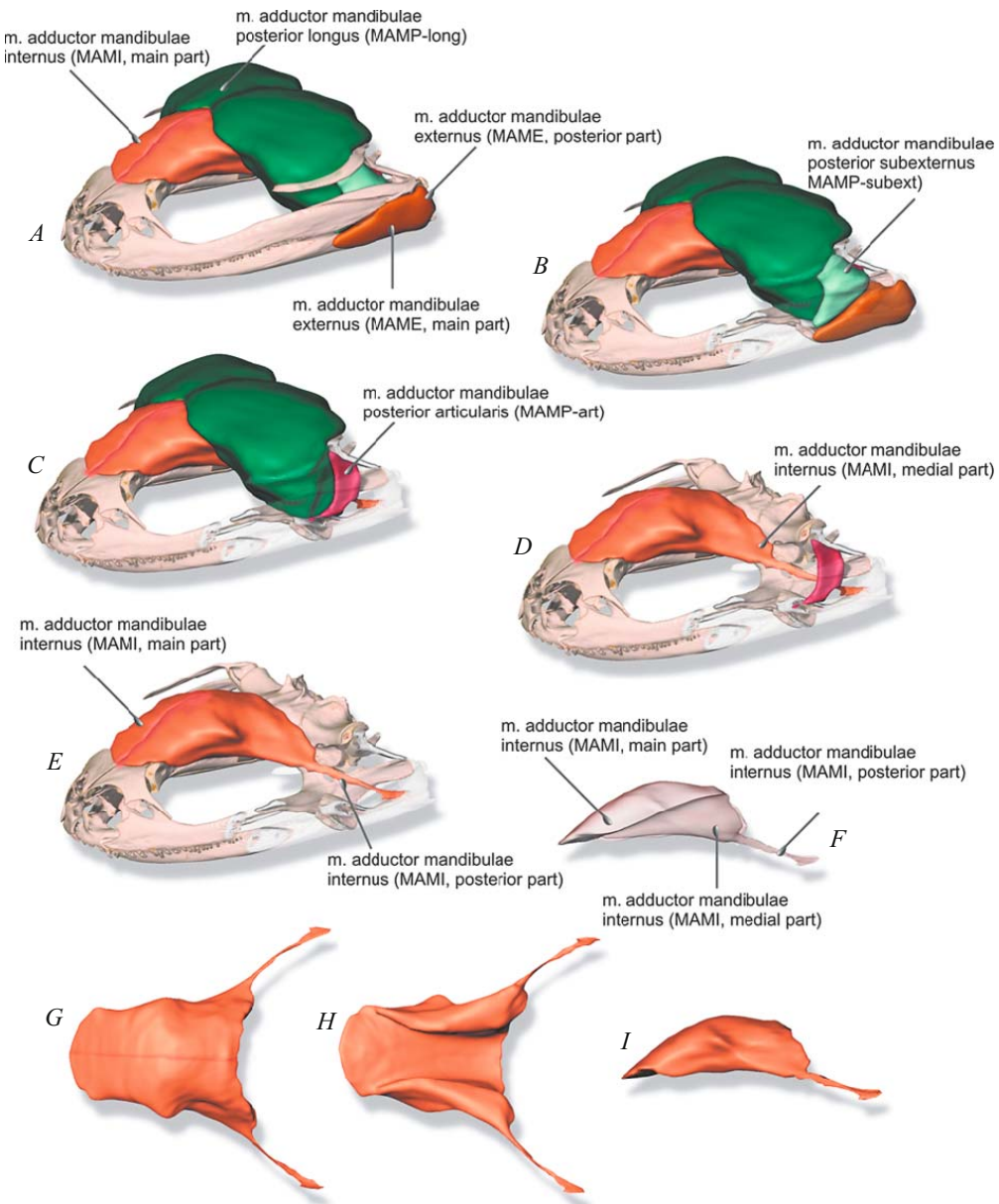

Fig. 10. Three-dimensional reconstructions of jaw adductors of fully grown *Barbourula busuangensis* (ZRC 1.10828; synchrotron x-ray images) and their topographic relationships with the skull: *A*, complete system and its relations to jaws and squamosal; *B*, complete system of adductors after removal of posterior parts of jaws. Note functional complex of MAMP-long, MAMP-subext, and MAME (compare Fig. 9*A*); *C*, same as in (*B*), but MAMP-subext removed (compare Fig. 9*B*); *D*, same as in (*C*), but MAMP-long removed. Note courses of posterior parts of MAMI and MAMP-art (compare Fig. 9*C*); *E*, same as in (*D*), but MAMP-art removed; *F*, Right MAMI in medial aspect; *G*, *H*, both MAMI in dorsal and ventral aspects; *I*, left MAMI in lateral aspect (compare Fig. 9*E*). Note that MAMI is not subdivided in fully grown individuals; *A* – *E*, in same aspects as in Fig. 9*A* – *C*. Posterior parts of jaws removed in (*B* – *E*).

antero-laterally into the posterior part of the orbit, where it turns ventrally and inserts on the medial surface of the lower jaw.

In *Barbourula busuangensis*, MAMP-subext inserts on MAME (Figs. 9*A* and 10*B*), either on its medial surface or, anteriorly, on its dorsal surface. It adjoins the lateral fascia of MAMP-long, and the parallel course of fibers of both muscles suggests that both have the same function. It originates from the inner surface of the lamella alaris squamosi (Fig. 10*A*). Posteriorly, it adjoins the anterior wall of the Eustachian tube.

MAMP-art (Figs. 9*B*, *C* and 10*C*, *D*) is a short but strong muscle located close to the jaw joint between MAMP-subext and the insertion of MAMP-long. Its posterior part is stretched between the ventral surface of the palatoquadrate and Meckel's cartilage, whereas its anterior portion lies between the ramus paroticus squamosi and the angulare. Anteriorly, it terminates at the level of the otic articulation (Fig. 9*C*).

MAMP-long is the principal muscle of the adductor mandibulae posterior group, and the main adductor of the mandible. It has a narrow, antero-posteriorly elongated insertion on the angulare, medial from the insertion of MAMP-art and below the insertion of MAMI. Further anteriorly it runs below the palatoquadrate, where it is attached to the fascia of MAMI. Below the Eustachian tube it is robust and well separated both from MAMP-art and MAMI. It emerges from below the crista parotica in the orbit, where it turns dorsally and passes onto the roof of the otic capsule, where it runs posteriorly and posteromedially. It originates on the spikes and cristae of the parietal portion of the frontoparietal and adjacent areas of the otic capsule.

In the sectioned subadult female specimen (DP FNSP 6582), MAMI consists of three parts (Fig. 9*E*): an anterior, robust main part, a middle part, and a posterior part. The main part begins as a thin and narrow sheet above the medial margin of the nasal, separated from its counterpart on the opposite side by a thin aponeurosis. It gradually becomes broader posteriorly, and at the level of the anterior end of the frontoparietal it extends beyond the lateral margin of the braincase. It is isolated from the nasals in the subadult female, which might be an artifact, and becomes attached to the skull roof along the midline only at the level of the anterior end of the frontoparietals (Fig. 5*F*, *G*). Here, its fibers are oriented antero-posteriorly. Further posteriorly, its lateral margin is deflected ventrally (Figs. 8*B* – *D*, 9*A* – *D*, and 10*A* – *E*, *H*) and muscles of both sides originate exclusively from the median aponeurosis. The posterior part of the main portion of MAMI terminates within a fascia that continues onto the middle part of MAMI.

The middle part of MAMI begins as a thin sheet adjoining the lateral wall of the braincase, covered laterally by the main part (Fig. 8*D*). It originates on the median aponeurosis by means of a delicate but well discernible tissue layer (Fig. 8*E*). The middle part of MAMI then runs horizontally and becomes attached to the fascia where the main part of MAMI terminates. This fascia runs postero-ventrally as a thickened tissue layer (tendon, termed 'subarticular aponeurosis' by Iordansky, 1996) along the medial surface of MAMP-long. It then passes below the crista parotica and palatoquadrate, and runs parallel and dorsal to MAMP-long where the latter becomes a thin bundle of fibers close to the medial surface of Meckel's cartilage. Ultimately, it has a common insertion with MAMP-art, but separate from MAMP-long, onto the medial surface of the angular, close to the jaw joint (Figs. 7*F*, 9*D*, and 10*E*).

Synchrotron x-ray imaging shows that MAMI was not subdivided in the fully developed adult specimen ZRC 1.10828 (Fig. 10), although the enormous extent of the muscle on the cranial roof is similar to DP FNSP 6582. This suggests that in ZRC 1.10828 the separate parts of the MAMI fused together, or that the synchrotron x-ray imaging was unable to record the delicate details of MAMI muscular anatomy (Fig. 3). Ontogenetically, the cascade-like structure of MAMI, consisting of three discrete units (Fig. 9*C* – *E*) in the subadult *Barbourula* specimen (DP FNSP 6582), may fuse later in life (Fig. 10*I*), or the observed differences could reflect intraspecific variation or limitations of the imaging equipment.

Extrinsic eye muscles. The obliquus inferior muscle (MO-inf) originates on the braincase floor, close behind the postnasal wall (Fig. 11*A*). Its lateral portion, with fibers oriented transversely, is comparatively thick, whereas its medial portion is thinner and consists of antero-posteriorly oriented fibers. Both parts are easily distinguishable anteriorly, but become confluent posteriorly. The MO-inf adjoins the lower margin of the sclerotic cartilage, and inserts on the antero-medial surface of the eye bulb (Fig. 12*B*, *C*).

The obliquus superior muscle (MO-sup) originates immediately posterior to, but well separated from, the origin of MO-inf (Fig. 11*B*). Its anterior part inserts into the upper eyelid and its more posterior part onto the eye bulb.

The retractor bulbi mucle (MRB) is the most powerful of all eye muscles. Its origin extends from the anteromedial part of the lower surface of the ala parasphenoidei onto the cultriform process. The MRB runs anteriorly below the prootic fontanelle, where the basal articulation is impressed on its dorso-lateral surface (Fig. 12*C*). Further anteriorly, it is divided horizontally by a thin ligament of the rectus externus muscle (MR-ext; see below), attached to the lateral edge of the cultriform process of the parasphenoid (Fig. 11*H*, *I*). At the level of the optic foramen, the MRB spreads out to form a cone that inserts on the postero-medial surface of the eye bulb around the optic peduncle. The cone is interrupted medially by a passage for the optic nerve out of the interior of the cone. The lateral surface of the MRB is adjoined by a thick and broad tendon that bifurcates anteriorly; its dorsal portion runs around the inner surface of the eye bulb dorso-medially between the MO-sup and the levator bulbi (MLB) to insert in the upper eyelid. The ventral portion of the tendon

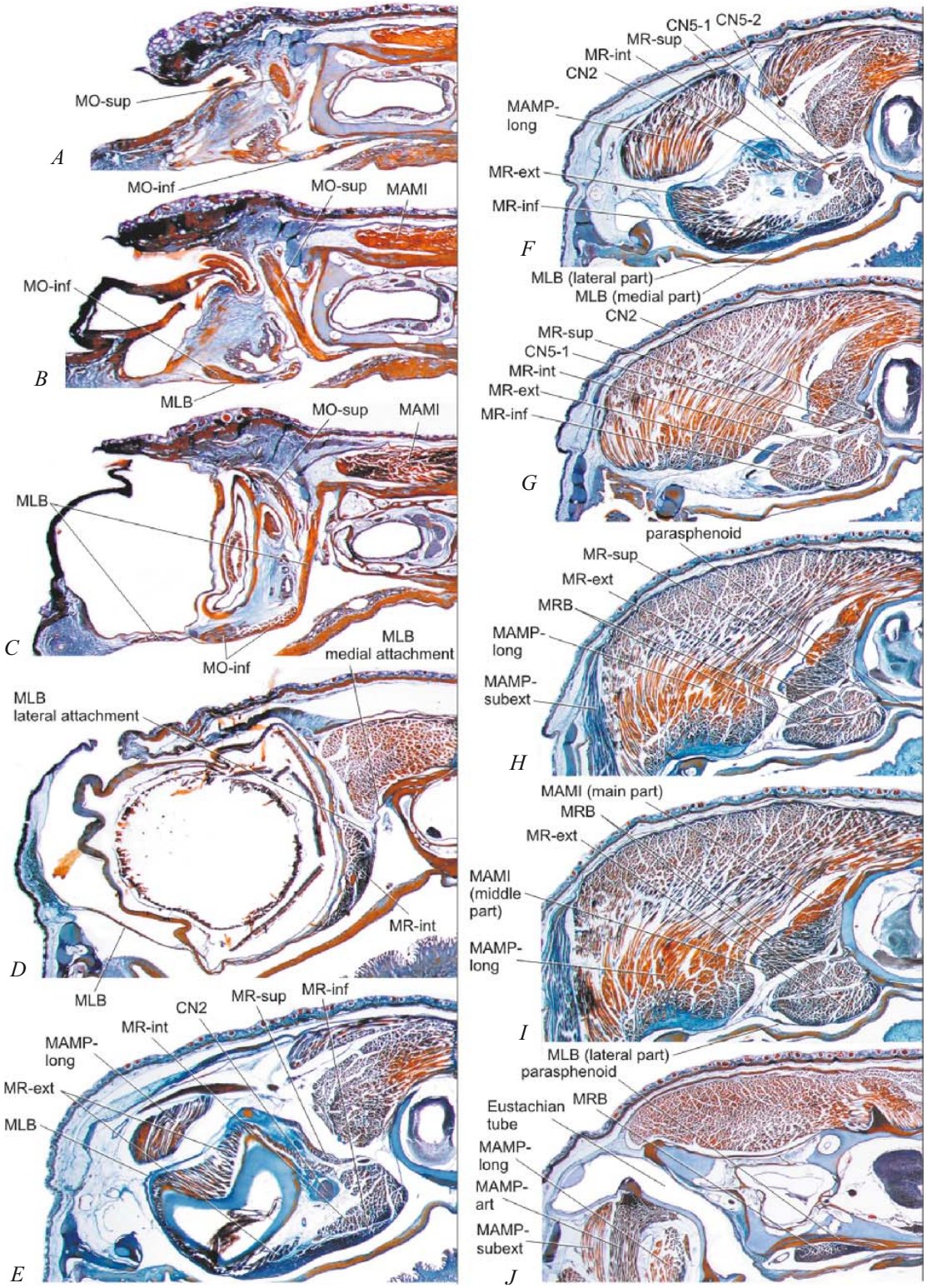

Fig. 11. Extrinsic eye muscles of *Barbourula busuangensis* (DP FNSP 6582) as revealed in transverse sections: *A*, origin of MO-inf on basis of braincase; *B*, origin of MO-sup on basis of braincase, posterior to MO-inf; *C*, anterior attachments of MLB; *D*, medial attachments of MLB and anterior termination of MR-int; *E*, arrangement of eye-muscles around posterior end of eye bulb; *F*, arrangement of eye-muscles in posterior part of orbit; *G*, anterior division of MRB; *H*, relation of MR-ext to MRB; *I*, origin of MR-ext; *J*, origin of MRB. Only left parts of sections are illustrated.

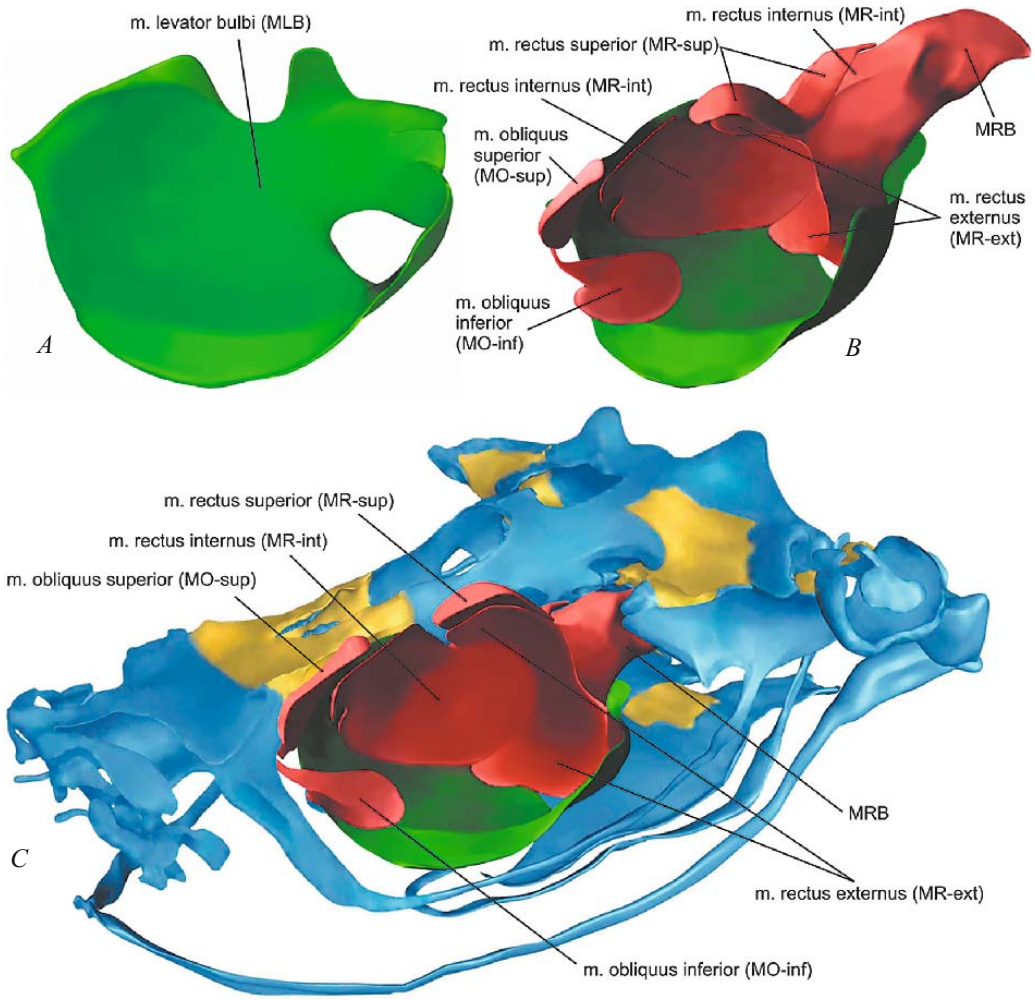

Fig. 12. 3D reconstructions of extrinsic eye muscles of not fully grown *Barbourula busuangensis* (DP FNSP 6582): *A*, isolated left MLB; *B*, isolated extrinsic muscles of left eye; *C*, extrinsic eye muscles in skeletal context. All are in same view as in Figs. 6*A* and 9*A* – *D*. Color code of endoskeletal structures same as in Fig. 6.

runs medially over the surface of the cone, ultimately dividing the most anterior part of the cone into thin dorsal and ventral parts. The tendon then continues to the anterior corner of the eye, where it merges with the nictitating membrane.

The rectus externus muscle (MR-ext) originates from a thin, flat tendon from the lateral edge of the cultriform process (Fig. 11*H*), anterior to the origin of the MRB. Its posterior part is completely surrounded by MRB, but it then runs anterolaterally within the MRB. Where the MRB begins to spread out into a cone, the MR-ext appears on its surface (Fig. 11*F*). Here it is supplied by a terminal branch of CN6. The MR-ext then expands as a thin horizontal sheet around the posterior part of the eye bulb. Because the MRB also expands laterally, both fuse into a single layer, in which MR-ext loses its identity.

The rectus internus muscle (MR-int) originates from the perichondrium of the ventral part of the braincase behind the optic foramen and extends anteriorly between the MRB (impressed in its medial surface) and the braincase. It inserts on the medial surface of the eye bulb, anterior to the optic peduncle.

The rectus inferior muscle (MR-inf) originates in the same area as the MR-int, but more ventrally, in a tissue layer adjoining, but not directly attached to the lateral margin of the cultriform process of the parasphenoid. Although their origins seem to be confluent, the MR-inf and MR-int can be recognized by the orientation of their fibers. MR-inf runs from its origin antero-laterally as a comparatively thick layer between the MLB and the cone of the MRB, and terminates approximately at the level at which the optic nerve leaves the eye bulb, without di-

rectly inserting on its surface. It is the smallest of all the extrinsic eye muscles.

The rectus superior muscle (MR-sup) originates in a strip of tissue attached to the lateral margin of the cultriform process of the parasphenoid (Fig. 11*H*). It runs anteriorly along the lateral surface of the braincase towards the ventral margin of the optic foramen, where it passes between the optic nerve and CN6 (Fig. 11*G*). Ultimately, it expands onto the dorso-medial surface of the eye bulb, where it partly covers the end of the MR-ext (Figs. 11*E* and 12*B*, *C*), and inserts on the dorso-medial surface of the eye bulb.

The levator bulbi muscle (MLB; Fig. 12*A*) in the subadult female (DP FNSP 6582) is represented by a thin sheet which lies between the eye bulb and the roof of the mouth cavity; thus it forms the elastic floor of the orbit. Its medial margin, thick anteriorly, is attached to the frontoparietal (Fig. 11*C*). Further posteriorly, it becomes thinner and splits into two divergent layers. The lateral layer inserts in a tissue that covers the main part of MAMI, while the medial layer is attached to the frontoparietal (Fig. 11*D*). Within the majority of the orbit, MLB is a uniformly thin aponeurosis devoid of any muscle fibers. Further posteriorly, muscle fibers re-appear, but MLB is still extremely thin, although it increases in thickness laterally. Below the posterior end of the eye bulb, MLB splits into two portions, the medial one partly overlapping the lateral one (Fig. 11*F*). The medial portion also terminates more posteriorly than the lateral one, and is involved in the horizontal tissue layer stretched between the cultriform process of the parasphenoid and the subocular bar.

DISCUSSION

Barbourula is similar in many skeletal features to the early Cretaceous anuran *Liaobatrachus* Ji and Ji, 1998, which is represented by several tens of extraordinary well preserved fossils from the late Early Cretaceous (Lower Aptian, slightly older than 125 Ma) of Liaoning Province, northeast China (Clarke, 1987; Roček et al., 2012; Dong et al., 2013). These similarities include a deep and anteriorly bifurcated maxilla, basal articulation preserved as a movable joint, V-shaped parahyoid, ossified posteromedial processes of hyoid, imbricate neural arches, free ribs with uncinate processes on the 2nd, 3rd, and 4th presacral vertebrae, broadly dilated sacral diapophyses, and a monocondylar sacro-urostylar articulation. *Liaobatrachus* is one of only a few articulated Mesozoic anurans known (all others are represented by isolated bones), and the only Mesozoic frog that is represented by 3D preserved adults (3D preserved pipoid tadpoles are known from the Early Cretaceous of Israel (Roček and Van Dijk, 2006). It is therefore interesting to compare skeletal features of the extant basal anuran *Barbourula* with well preserved, more than 100 million years old frogs.

***Barbourula* and *Liaobatrachus* — comparisons between an extant basal frog and a frog from the Cretaceous.** Although most of internal structures of the head and the muscles are not preserved in *Liaobatrachus* from the Early Cretaceous (131 – 120 Ma) of China, some overall comparisons between *Barbourula* and *Liaobatrachus*, which are separated by at least 125 Ma, can be made.

Barbourula resembles *Liaobatrachus* in the suite of following features: Nasals meet in a long median contact; maxilla is deep and bifurcated anteriorly, receiving lateral end of the premaxilla in the depression between the dorsal and ventral processes (Fig. 4*D*; Dong et al., 2013: Fig. 3*C2*, 7*D*); lamella alaris squamosi and maxilla are separated (because maxilla is without processus zygomatico-maxillaris); ramus paroticus of the squamosal is absent (Fig. 4*B*; Dong et al., 2013: Fig. 7*D*); processus frontalis of the maxilla is pointed (because nasal and maxilla meet in an oblique suture; Fig. 4*D*); basal articulation is preserved as a movable joint, evidenced by the pars medialis of the pterygoid deflected from the prootic (Fig. 4*D*, *K*; Dong et al., 2013, Fig. 6*B*), whereas it is fused, e.g., in *Pelobates* (Roček, 1981), *Rana* (Pusey, 1938), and *Bufo* (Ramaswami, 1937); long anterior fontanelle is between paired frontoparietals (present in adult *Liaobatrachus* and immature *Barbourula*); columella is present; mentomeckelian bones are present (Dong et al., 2013, Fig. 7*E*), also, e.g., in *Scaphiopus* (Hall a Larsen 1998); V-shaped parahyoid is present (Fig. 4*I*; Dong et al., 2013), also in *Pelobates* (Roček, 1981) and in some discoglossids (Roček, 2003), absent in *Bombina* (Slabbert, 1945); posteromedial processes of hyoid is ossified (Fig. 4*I*; Dong et al., 2013); free ribs are present on the 2nd – 4th vertebrae; ribs on the 2nd vertebra are terminated by transverse processes directed anteriorly and posteriorly ("hatchet-like" rib; Clarke, 1987: Figs. 8 and 9; Dong et al., 2013); ribs on the 3rd vertebra are with uncinate process; transverse processes of sacral vertebra is broadly dilated, fan-like; neural arches are strongly imbricate; sacro-urostylar articulation is monocondylar (Clarke, 1987); urostyle is provided with a pair of transverse processes (also, e.g., in *Gobiates*; Roček and Nessov, 1993; Roček, 2008); ilium lacks dorsal tubercle.

The combination of these features may be considered characteristic for Mesozoic anurans and extant taxa that display a similar set of characters may be considered basal in their phylogenetic position.

On the other hand, *Barbourula* differs from *Liaobatrachus* in having a lower number of presacral vertebrae

(8 vs. 9, respectively), and opisthocoelous vertebral centra (instead of amphicoelous in *Liaobatrachus*). These two features are important differences, but the first may be explained by the aquatic lifestyle of *Barbourula* (permanent water-dwellers, such as pipids and palaeobatrachids, show tendency to reduction of number of vertebrae (e.g., Estes, 1977; Špinar, 1972), and the second by the fact that opisthocoelous and procoelous vertebrae evolved from the amphicoelous condition by the end of Mesozoic in anurans (Roček et al., 2010). The earliest opisthocoelous anuran vertebrae are known from the earliest Cretaceous of Israel (Nevo, 1968), and the earliest procoelous vertebrae from the earliest Cretaceous (possibly Berriasian) of Morocco (Jones et al., 2003; Rage and Dutheil, 2008) and from the early Cretaceous (Albian) of Texas (Winkler et al., 1989).

Connections of the palatoquadrate. The palatoquadrate and Meckel's element are principal jaw components of gnathostomes. In amphibians, both remain cartilaginous, except for little ossifications (quadrate and articulare, respectively) which form the jaw joint. In Devonian ancestors of tetrapods, the palatoquadrate was ossified, free, and connected to the neurocranium by several articulations. In amphibians, including temnospondyl ancestors of anurans, some of these articulations became immovable connections, generally termed "commissures" (which means a line or place at which two things are joined; Wu et al., 2012), but mostly described under their specific names (Shishkin, 1973; Reiss, 1997). One of such immovable connections of the anterior part of the amphibian palatoquadrate is the commissura quadrato-cranialis anterior (direct connection to the lateral wall of the braincase) and two quadrato-ethmoidal commissures (connections to the posterior wall of the nasal capsule, the medial one, and lateral one). Because ossification of the palatoquadrate and Meckel's element in adult amphibians was arrested at cartilaginous level, we can infer their shape and location only from imprints on the inner surface of dermal bones. This is why very little is known about the early stages of temnospondyl larvae; their earliest fossilized stages with preserved bones are only from metamorphosis (Schoch, 1992). Nevertheless, comparisons of skulls of young and adult individuals of branchiosaurs (Boy, 1978) revealed different positions of the quadrate relative to the otic capsule, possibly caused by rotation of the palatoquadrate posteriorly (see also Roček, 2003: Fig. 62), similar to metamorphosing anuran tadpoles (see below).

In early development of anuran larvae, the palatoquadrate and Meckel's cartilage first rotate from their original vertical position anteriorly to the horizontal position and the palatoquadrate becomes connected to the cranial trabecle, just behind the nasal capsule, by the commissura quadrato-cranialis anterior (e.g., Spemann, 1898). Due to this rotational shift, Meckel's cartilage remains short in anuran tadpoles and, more importantly, larval jaws are represented by elements (upper and lower labial cartilages) that are different from those in adults. During metamorphosis, the palatoquadrate and Meckel's cartilage rotate posteriorly below the otic capsule. Meckel's cartilage becomes elongated and takes over the function of the lower jaw. Consequently, the jaw joint is located beneath the posterior part of the otic capsule. In addition, direct connection of the palatoquadrate to the braincase becomes interrupted, the vestigial quadrato-cranial commissure (called the subocular bar by some authors) becomes connected to the nasal capsule only via quadrato-ethmoidal commissures, as evidenced by *Ascaphus* (van Eeden, 1951), and supports the maxilla. As a consequence of all these processes, the palatoquadrate comes in contact with the otic capsule where a new connection is established, called the otic articulation (Pusey, 1938; Ramaswami, 1940; Barry, 1956). In our sectioned specimen of *Barbourula*, the connection between the palatoquadrate and crista parotica of the otic capsule is a thin cartilaginous bridge (Fig. 7*B*). The cartilaginous crista parotica is histologically distinguishable from the capsule, which was also cartilaginous in our not fully grown female (Fig. 7*B*, *C*). This indicates that the crista does not develop from the capsule (see also de Villiers, 1934, Fig. 7*D*; Swanepoel, 1970), but is formed by condensation of cartilaginous cells from the disintegrated hind end of the larval palatoquadrate (van der Westhuizen, 1961).

The otic articulation was not visible in the articulated skulls of our two fully developed adults, but the crista parotica and otic process are probably fused with one another, as in *Ascaphus*, *Leiopelma*, and *Bombina* (de Villiers, 1934; Stephenson, 1951), even though the two structures might still be distinguishable histologically.

Another connection of the palatoquadrate with the otic capsule is the basal articulation. Its terminology in temnospondyl amphibians varies in accordance with its position and components — whereas primarily it is a potentially movable articulation between the basal process of the palatoquadrate and the basipterygoid process of the prootic, these two processes may secondarily fuse together and, in addition, to involve the parasphenoid and the pterygoid, thereby causing immobility in the articulation.

It follows from what was said about the transformation of the mouth apparatus in the anurans that also the basal articulation is established only in course of metamorphosis. In our sectioned specimen of not fully grown *Barbourula* DP FNSP 6582, it preserves the structure of a true joint (Figs. 7*A* and 8*I*), whereas in the majority of

other anurans it shows various levels of fusion. The connection by means of a joint with a preserved joint cavity occurs not only in the subadult, but also in fully grown *Barbourula*, as indicated by prominences on the anterior surface of the prootic, covered by a funnel-like extension on the medial ramus of the pterygoid in DP FNSP 6554 (Fig. 4*D*) and ZRC 1.10828 (Fig. 4*K*). However, the potential movability of this joint in *Barbourula* is hindered by increased overlap of the parasphenoid ala by the medial ramus of the pterygoid with increasing size of individuals (Clarke, 1987). A similar joint with a preserved joint cavity was observed in adult *Bombina bombina*. In adult *Heleophryne purcelli*, the basal process leans against the anteroventral surface of the otic capsule, but does not fuse with it (van der Westhuizen, 1961: Fig. 40). In adult *Rana* (Pusey, 1938) and *Pelobates fuscus* (Roček, 1981), both processes are confluent. Thus, among various anuran taxa, a developmental (and evolutionary) sequence may be inferred, from the typical structure of a joint (*Barbourula*, *Bombina*), through a mere contact between both processes (*Heleophryne*), up to immovable fusion (*Rana*, *Pelobates*). The absence of the basipterygoid process in *Leiopelma* (Stephenson, 1951) is probably associated with its hypo-ossification.

Jaw adductors and anuran evolution. The basal phylogenetic position of *Barbourula* among extant anurans may be inferred not only from comparisons of its skeletal features with Cretaceous *Liaobatrachus* and from molecular studies (Fig. 13; Blackburn et al., 2010), but also from the arrangement of its jaw adductors.

Attempts to reconstruct jaw adductors in ancestral temnospondyls were made by Säve-Söderbergh (1945) and Carroll and Holmes (1980), however, with only tentative results. Both stressed that the jaw adductors must have originated within a limited space of the adductor chamber completely covered dorsally by dermal bones. Säve-Söderbergh (1945) inferred muscle attachments from tuberosities on inner skeletal surfaces of the chamber. He found one such attachment area along a crest on the underside of the skull roof just laterally to the side wall of the orbito-temporal region of the endochondral braincase (for his m. pseudotemporalis superficialis; Table 2), and in a roughened area at the junction of the dorsal end of the epipterygoid and the side wall of the braincase (for his m. pseudotemporalis profundus). These muscles are undoubtedly parts of the MAMI complex. In addition, another muscle, which he homologized with the MAMP group, originated from the posterior part of the palatoquadrate. None of these adductors could have originated from the otic region, because the otic capsules were tightly adhered by dermal bones. All had to insert on the coronoid process. Carroll and Holmes (1980) supposed that jaw adductors were arranged in three major divisions as in living caudates, and restored their origins and insertions in two small labyrinthodonts, *Dendrerpeton* and *Doleserpeton*, on the basis of their typical areas in living lower tetrapods. They inferred the origin of MAMI from the lateral wall of the braincase, limited anteriorly by the level of the anterior margin of the orbit, and posteriorly by the epipterygoid and prootic. They were not able to recognize a superficial and profundus head of MAMI, but they attempted to illustrate this subdivision in their Figs. 25 and 26. The MAME was in the most external position, and would have originated on the upper cheek region between the orbit and the otic notch. The MAMP was limited laterally by MAME, anteriorly by MAMI, and its origin was inferred after the quadrate ramus of the pterygoid (terminology after Carroll and Holmes, 1980).

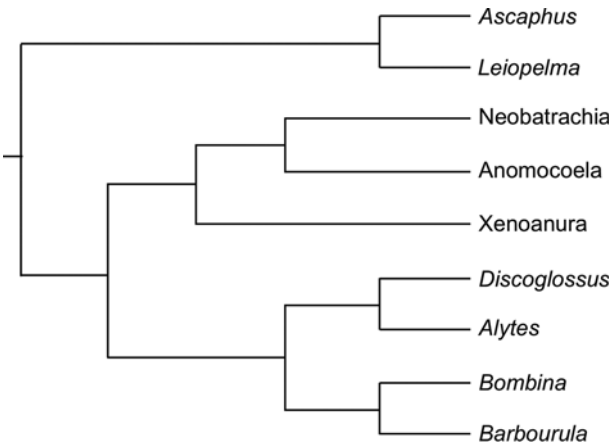

Fig. 13. Hypothetical phylogenetic relationships of *Barbourula*, based on molecular data. From Blackburn et al. (2010).

In caudates, which are the closest relatives of the anurans, MAME is large and typically originates from the squamosal and palatoquadrate, with tendency to expand its area of origin to the fascia of the m. depressor mandibulae, prootic and parietal. It inserts on the dorsal and lateral surfaces of the lower jaw (Luther, 1914; Carroll and Holmes, 1980). It is a single muscle in primitive living caudates (e.g., *Hynobius*), but may be further subdivided in larger ones (e.g., *Cryptobranchus*; Fig. 14). MAMP is a small muscle, either single or divided in three heads (subexternus, articularis and longus). All these heads originate from the squamosal and palatoquadrate, medial to MAME, the subexternus head being the most lateral and the articularis head the most medial. The subexternus head inserts on the coronoid process and the articular, the longus head on the tendon of the m. pseudotemporalis or directly on the jaw in its vicinity, and the articularis head on the medial surface of the articular. MAMI consists of two discrete portions: the pterygoide-

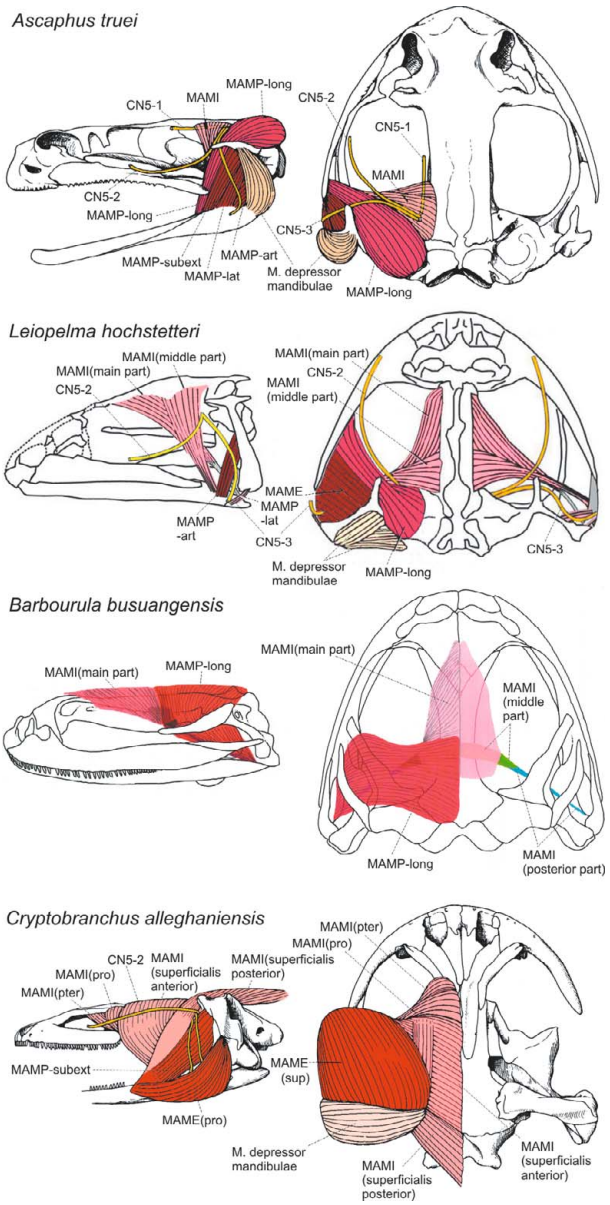

Fig. 14. Dorsal and left lateral views of the skull in *Cryptobranchus*, a primitive extant caudate, and in basal extant anurans *Barbourula*, *Leiopelma*, and *Ascaphus*, showing patterns of MAMI. *Cryptobranchus* may indicate a possible original lissamphibian pattern, anurans gradual exposure of skull roof (not necessarily in phylogenetic sequence). Note large MAME, consisting of two heads in *Cryptobranchus*, whereas it is strongly reduced in anurans (not shown in *Barbourula*, but see Fig. 9*A*). Reduction of MAMI results in exposure of skull roof, and the main role among jaw adductors is taken over by MAMP-long. *Ascaphus* and *Cryptobranchus* reproduced from Carroll and Holmes (1980), *Leiopelma* from Johnston (2011), *Barbourula* after DP FNSP 6554 and 6582.

us portion anteriorly (which may extend up to the nasals, as is the case with *Cryptobranchus*; Carroll and Holmes, 1980), and the pseudotemporalis portion posteriorly; the latter is further subdivided into the anterior, profundus head and the posterior, superficialis head. The superficialis portion is sometimes subdivided into an anterior and posterior parts (Fig. 14). Despite the separate origins of the caudate pterygoideus and both pseudotemporalis heads, their insertion tendons tend to fuse with each other distally, and this is probably why Luther (1914) considered them to be part of a single adductor. It was once believed that MAMI in the anurans represents the pterygoideus of the caudates (Luther, 1914; Gaupp, 1896; Lubosch, 1938), but this was later refuted (Carroll and Holmes, 1980). MAMI may be a single, not subdivided muscle originating from the lateral edge of the frontal and parietal or, when the pterygoideus head is differentiated from the pseudotemporalis head, the pterygoideus head originates from the lateral edge of the frontal and the pseudotemporalis head (or its subdivisions) from the parietal. Both the pterygoideus and pseudotemporalis head (and subdivisions of the latter) insert by separate tendons onto the dorsomedial surface of the coronoid process and adjacent parts of the jaw ramus. The posterior parts of MAMI (but also all three heads of MAMP and deep head of MAME) run anteroventrally. It may be also of some importance that the origin of the pterygoideus head tends to migrate ventrally, below the pseudotemporalis head, but it still originates from the frontal and parietal (Carroll and Holmes, 1980).

The origin of frogs was associated with a marked shortening of the otic region of the skull, which can be already seen in *Triadobatrachus*, a proanuran amphibian from the early Triassic (Induan, about 250 Ma) (Rage and Roček, 1989). This inevitably resulted in a distinct change in muscle orientation. Those adductors which were directed from their origins to insertions anteroventrally in ancestral temnospondyls (judging by situation in living caudates) run posteroventrally in anurans. Little can be added to what was already mentioned by Carroll and Holmes (1980). MAME and MAMP-lat became strongly reduced and may be even absent in the anurans; the most important of the jaw adductors became the longus head of the MAMP, and its origin migrated from the adductor chamber onto the dorsal surface of the otic capsule; origins of all MAMI portions either were reduced on the anterior (frontal) part of the frontoparietal, or moved posteriorly, onto the lateral edge of the posterior (parietal) part of the frontoparietal. The skull roof became exposed and is covered only by skin.

It is of interest to examine the jaw adductors of *Barbourula* (which is similar to the early Cretaceous anuran *Liaobatrachus* in many aspects) in the context of currently accepted phylogenies (Cannatella, 1985; Gao and Wang, 2001; Blackburn et al., 2010; Pyron and Wiens, 2011; Dong et al., 2013). All of these, whether they are

based on molecular or available morphological data, present *Barbourula* and *Bombina* as sister taxa, both most closely related to a clade comprising *Alytes* and *Discoglossus* (Fig. 13). *Leiopelma*, which is a member of the clade *Ascaphus* + *Leiopelma*, is generally considered to be the sister taxon to all other living anurans, is considered more distantly related to *Barbourula*. Therefore, in the descriptions below, we first assess the condition in *Bombina*, *Alytes* and *Discoglossus*, and then in other extant basal frogs.

In *Barbourula*, MAME is vestigial but still present, although as a part of more complex unit. It has also been identified in larval *Bombina* and *Alytes* (Haas, 2001: Figs. 1, 2) and in postmetamorphic *Bombina* and *Discoglossus* (Haas, 2001: Fig. 13). It is not clear whether it persists in adult *Alytes*. It is present in larval and adult *Ascaphus* (Pusey, 1943; Haas, 2001: Fig. 12; Johnston, 2011) and in adult *Leiopelma* (Stephenson, 1951; Johnston, 2011). The m. adductor mandibulae lateralis of Iordansky, situated 'laterally under the jugal arch' (Iordansky, 1996: 11, Fig. 2*a*) was considered an isolated, posterior portion of MAME (Iordansky, 1991, 1992). In *Barbourula*, it is represented by an outer layer of MAME, stretched between the quadratojugal and angular and clearly distinguishable by course of its fibers. It lost its function not only because it has no dorsal skeletal attachment (thus, it became part of the body of MAME), but also because it was pre-destinated for it by location of its origin and insertion close to the jaw joint. Among anurans, the presence of MAME is clearly a primitive feature. Its presence in the larvae of basal anurans, but absence or reduced size in adults, suggests that the role of this muscle has decreased or was taken over by other muscles in the adult. However, because the MAME in *Barbourula* (and possibly also in other frogs) constitutes a functional unit with other muscles (such as MAMP-subext and MAMP-long), it should not be considered in isolation, but rather in the context of other muscles. Taking this into account, vestigial MAME can be considered a ventral portion of a complex adductor, the dorsal part of which is MAMP-subext; MAMP-subext, in turn, is attached to the fascia of MAMP-long and to the anulus tympanicus and squamosal, as is the case with fully developed MAME. It should be added that vestigial MAME, considered separately from other muscles, would be non-functional, because it has no dorsal skeletal attachment; instead, it is attached to a fascia of MAMP-subext (Fig. 7*A – D*).

In most anurans, MAMI is reduced and less well developed than in caudates. Generally, it is a single muscle which originates from the lateral margin of the frontoparietal and lateral wall of the braincase at the level of the posterior part of the orbit, sometimes also from the antero-ventral surface of the prootic, leaving the skull roof exposed. The proximal, fleshy part of MAMI tapers distally and continues as a long, ribbon-like tendon (termed 'coronar aponeurosis' by Iordansky, 1996) along the medial surface of MAMP-long posteroventrally and almost laterally towards the medial face of the coronoid process where it inserts. This transverse course (Fig. 14) is obviously associated with antero-posterior abbreviation of the otic region of the skull, and because it is unlikely to generate significant force for adducting the lower jaw, it suggests loss of importance of MAMI among jaw adductors. In *Bombina* (Fig. 15), *Discoglossus*, and *Alytes*, MAMI neither extends onto the skull roof, nor is it subdivided into a cascade-like succession of several portions, as is the case in subadult *Barbourula*.

The complete coverage of the interorbital portion of the skull roof by the robust anterior part of MAMI in *Barbourula* is reminiscent of primitive caudates such as *Cryptobranchus* rather than anurans (Carroll and Holmes, 1980: Fig. 20). The most similar to *Barbourula* is the arrangement of MAMI in *Leiopelma*, one of the most basal extant anurans. In *Leiopelma*, the origin of MAMI extends far anteriorly, up to the anterior end of the frontoparietal (Johnston, 2011), i.e., farther than in *Ascaphus* and in most other frogs, but less far anteriorly than in *Barbourula* (Fig. 14). In *Leiopelma*, MAMI is composed of two parts discernible by manual dissection, merging into one another: a rostral part, in which the fibers originate on the lateral edge of the frontoparietal but converge posteriorly onto a flat tendon, and a caudal part with a more ventral fiber direction (Fig. 14; Johnston, 2011). On the other hand, *Leiopelma* differs from *Barbourula* in an incomplete coverage of the skull roof by MAMI, and by insertions of the both parts of MAMI — whereas the anterior portion of MAMI inserts by a tendon on the mandible immediately medial to its articulation with the quadrate, the posterior portion of MAMI has a fleshy insertion adjacent to the tendon of the anterior part. Thus, *Leiopelma* has no cascade-like structure and both parts of its MAMI insert independently, but close to each other. Johnston (2011) termed both parts of MAMI in *Leiopelma* the adductor mandibulae internus rostralis and adductor mandibulae internus caudalis (Table 2) and considered them both homologous with the m. pterygoideus of Luther (1914) or m. pseudotemporalis of Iordansky (1996). As regards *Barbourula*, it may be hypothesized that, judging by the area of its origin, the middle portion of MAMI is a homolog of m. pseudotemporalis, which inserts by a thin aponeurosis provided with some, probably residual, muscle fibers, to the lower jaw. Hypothetically, and because the muscle fibers obviously have no or limited function (similar to, e.g., m. tensor fasciae latae), this posterior part of MAMI could be a

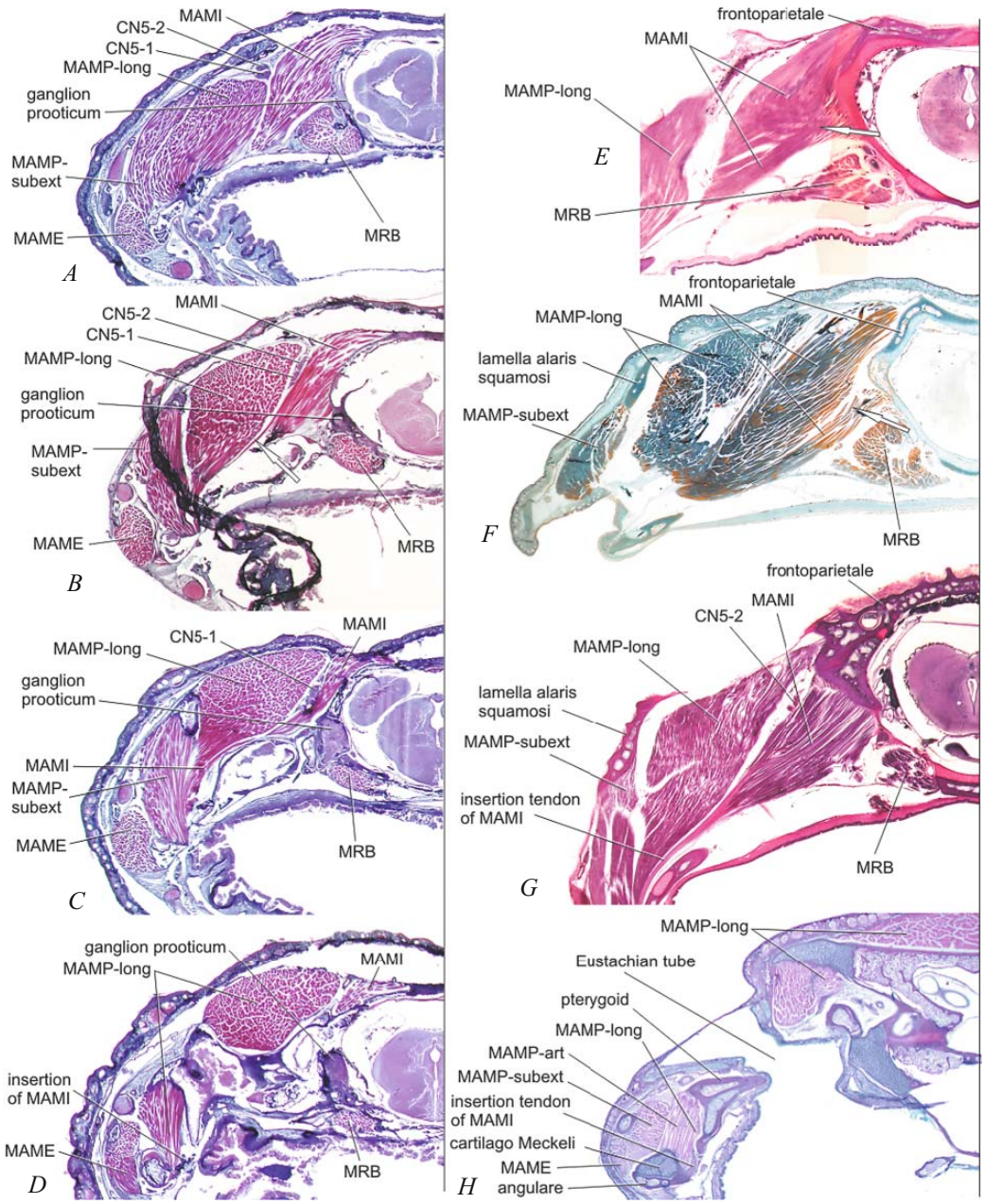

Fig. 15. Transverse sections through the skull of *Bombina bombina* (*A* – *D*), *Rana esculenta* (*E*), *Rana temporaria* (*F*), *Pelobates fuscus* (*G*), and *Hyla arborea* (*H*) to show MAMI and its relations to neighboring muscles: *A*, *E*, *F*, *G*, anterior part of MAMI and its attachment to frontoparietal and braincase. Separate, deep layer of MAMI in *Rana* is marked by arrows; *B*, superficial fibers of MAMI join medial surface of MAMP-long in *Bombina*; *C*, thin, posterior part of MAMI fuses with MAMP-long in *Bombina*; *D*, *H*, insertion of MAMI on medial surface of lower jaw in *Bombina* and *Hyla*, respectively. Only left parts of sections are illustrated. Not to the same scale.

vestigial superficial head of the pseudotemporalis. The main part of MAMI may be homologous with m. pterygoideus, because it originates above the nasals and frontals.

It may be objected that the similarities of *Barbourula* with *Leiopelma* in arrangement of MAMI do not reflect real phylogenetic relationships, and that departures of *Barbourula* from *Bombina*, *Alytes*, and *Discoglossus* may be due to its much more aquatic way of life, and possibly also due to eating hard-bodied prey such as crabs (Inger, 1954). A possibility of increasing of MAMI in size in *Barbourula* as a result of its food specialization

must be taken in account, but then it would be difficult to explain why it would return back to the complex subdivision rather than to a simple increase in size (similar to MAMP-long) from the condition found in *Bombina* and other closely related taxa, and why such an increase in size would not have been associated with strengthening of its coronar aponeurosis.

The most important adductor of the lower jaw in the Anura is MAMP-long. Generally, it originates on the dorsal surface of the otic capsule, runs along the anterolateral wall of the otic capsule, and inserts onto the coronoid process, close to the coronar aponeurosis of MAMI. Thus, its course is nearly vertical, which is very advantageous from the functional point of view. Moreover, its origin in *Barbourula* extends onto the parietal portion of the skull roof where it meets, similar to the main portion of MAMI, its counterpart from the opposite side of the skull. This covering of the skull roof extends anteriorly to the level of the posterior part of the orbit, so it partially covers the main part of MAMI (Fig. 14). It is not subdivided (Fig. 7), so in contrast to MAMI, MAMP-long of *Barbourula* may be considered secondarily increased in comparison with its relative size in its close relatives. The origin of MAMP-long is restricted to the roof of the otic capsule in adult *Bombina* and postmetamorphic juvenile *Discoglossus* (information on *Alytes* not available). MAMP-long originates exclusively from the roof of the otic capsule also in *Leiopelma* and *Ascaphus* (Johnston, 2011).

Remaining jaw adductors (MAMP-subext and MAMP-art) are rather uniform in all anurans, because they originate from the palatoquadrate and insert to the lower jaw, and their whole extent is in the interior of the adductor chamber. They run dorso-ventrally, and may be considered the most primitive of all adductors, because they are direct derivatives of the adductor mandibulae in ancestors of tetrapods.

Notes on intracranial relations of CN5 and CN7. In majority of anurans, the trigeminal and facial nerve ganglia fuse together before emerging from the braincase through a single prootic foramen, to form a single trigemino-facial (prootic) ganglion (Gaupp, 1899). In larval anurans, the ganglia are separated and fusion occurs in various stages of the late larval development and metamorphosis (Sokol, 1975; Fabrezi and Chalabe, 1997). However, *Leiopelma*, *Ascaphus*, *Discoglossus*, *Alytes*, and *Bombina* retain separate ganglia (and CN5 and CN7 even exit the braincase through separated foramina, separated by so-called prefacial commissure) until adult stage (Sokol, 1977).

In our not fully grown *Barbourula* female, CN7 does not enter the trigeminal ganglion and leaves the braincase through the dorsal portion of the prootic fontanelle, where it splits into the r. hyomandibularis and r. palatinus. This most probably represents the ultimate stage, similar to that found in *Bombina*.

Separate trigeminal and facial ganglia and the presence of a prefacial commissure are found in the caudates and apodans, and may be considered original tetrapod condition (Sokol, 1975). It seems that *Barbourula*, in which CN7 passes through the prootic fontanelle, is more derived than *Ascaphus* and *Leiopelma*, in which it passes through a separate foramen.

Extrinsic eye muscles. Compared with the caudates (e.g., Luther, 1914; Francis, 1934), the extrinsic eye muscles of frogs are less diversified. In *Barbourula*, two of them deserve a special note. MLB is located at the bottom of the orbit and it is just a thin aponeurosis with, or in some parts without, muscle fibers. Luther (1914) recognized three portions of this muscle in caudates — the sagittalis portion originating from the prootic and partly pterygoid, divided in the lateral and medial fascicles; the principalis portion originating from the parietal, frontal, prefrontal and postnasal wall, and inserting into the posterior part of the eyelid; and the transversalis portion, originating from the lateral edge of the parietal and frontal, and inserting on the maxilla or the eyelid. In most anurans, the sagittalis portion originates only from the prootic, and consists only of the medial fascicle. The principalis portion originates on the lateral edge of the frontoparietal, and inserts onto the zygomatic process of lamella alaris of the squamosal. The transversalis portion is poorly developed or absent; however, it is still well-developed in pre-metamorphic larvae (Luther, 1914: Fig. 17 – 20). It should be added that, according to Luther (1914), MLB arises in pre-metamorphic larvae as a narrow fascicle originating from the lateral wall of the braincase and inserting on the medial surface of the muscular process of the palatoquadrate above the system of antero-posteriorly oriented jaw adductors. Before metamorphosis, it differentiates into three portions, the more antero-posteriorly oriented transversalis portion, inserted on the commissura quadrato-cranialis anterior, the principalis portion, which is developmentally the earliest part of MLB stretched between the braincase and muscular process, and the sagittalis portion, oriented postero-laterally. During metamorphosis, the three portions enlarge their insertion areas and, due to disintegration of the muscular process of the palatoquadrate, the insertion of the principalis portion is shifted to the inner surface of the alar lamella of the squamosal. None of these portions can be discerned in immature *Barbourula* even on histological sections. The posterior ends of its two partly overlapping layers are free, without being attached to any skeletal structure. In contrast to *Barbourula*, MLB is

thick in *Bombina* and its parts are easily discerned (Iordansky, 1991; 1992).

MRB is a complex muscle which seems to occur in all tetrapods (Corning, 1902; Edgeworth, 1911; Bradley, 1933), occasionally including man (Whitnall, 1911; Krasny et al., 2011). It is generally defined as the most powerful of all the eye muscles, and originates from the lateral ala of the parasphenoid below the otic capsule, inserting as a cone on the medial surface of the bulbus oculi within the ring formed by the rectus muscles; the cone is interrupted by a slit through which the optic nerve passes from the eye bulb. This arrangement is similar in *Barbourula*. It has been known for a long time that MRB and MR-ext have the same topographic origin and share the same innervation (CN6; Neal, 1918). It seems that MRB arose in early tetrapods as a response to the need for eye retraction (i.e., as one of the adaptations to the terrestrial way of life), but not as a derivative of MR-ext, as suggested by developmental studies. Although MRB is absent from fishes, the coelacanth *Latimeria chalumnae* possesses a basicranial muscle stretching along the base of the neurocranium, reaching the posterior part of the orbit close to MR-ext (Millot and Anthony, 1965), and supplied by CN6 (Bemis and Northcutt, 1991). The same situation was inferred from the osteological arrangement in the Devonian basal sarcopterygian *Eusthenopteron foordi* (Jarvik, 1980). This is consistent with the conclusion reached by Bemis and Northcutt (1991) that MRB and basicranial muscles are homologous, and supports the view that MRB is a derivative of the basicranial muscle of the Devonian ancestors of amphibians.

The main function of MRB is retraction of the eye bulb, which may aid swallowing (Levine et al., 2004) and also forms, by means of a tendon that encircles the posterior part of the eye bulb, the motor apparatus of the nictitating membrane of the third eyelid (Whitnall, 1911; Lande and Zadunaiski, 1970).

CONCLUSIONS

The basal phylogenetic position of *Barbourula* within the Anura is supported by a cascade-like arrangement of MAMI, which consists of several parts. The arrangement of MAMI in *Barbourula* is reminiscent of the arrangement in primitive caudates and, to a certain degree, *Leiopelma*. A poorly developed MAME is also present in *Barbourula*, a muscle that has a variable distribution within the Anura. However, in anuran evolution there appears to be a tendency towards the formation of functional units from originally independent jaw adductor muscles (e.g., MAME + MAMP-subext or MAMP-long + MAMP-subext), and the reduced MAME of *Barbourula* should therefore not be considered in isolation. Other characteristics of *Barbourula* that reflect its basal phylogenetic position in Anura include the basal articulation, which preserves the structure of a true joint, even in fully grown adults, and the otic articulation, which is unfused, unlike the majority of extant anurans. The middle ear apparatus of *Barbourula* is complete. Of the extrinsic eye muscles, MLB is noteworthy because it is only a thin aponeurosis, and not differentiated into separate portions as is the case with other anurans. MRB, which main function is retraction of the eye bulb, is also well-developed in *Barbourula*. Unfortunately, comparative assessment of the extrinsic eye muscles in *Barbourula* is prevented by lack of corresponding data on other anuran taxa.

Acknowledgments. Thanks are due to Yuri A. van den Heever, Department of Botany and Zoology, University of Stellenbosch (South Africa), for providing the specimen of *Barbourula* now cataloged as DP FNSP 6582, and to Kelvin Lim and David Bickford, National University of Singapore (Singapore), for the loan of ZRC 1.10828. We are indebted to Wolfgang Maier, Department of Comparative Zoology, Institute for Evolution and Ecology (Germany), Eberhard Karls Universität Tübingen (Germany), for the use of laboratory facilities in his Department. Mikhail V. Mina, N. K. Koltzov Institute of Developmental Biology, Russian Academy of Science (Russia), is gratefully acknowledged for his valuable discussions on skeletochronology, and D. V. Shchepotkin for technical assistance. Jenny M. Narraway of Hubrecht Laboratory, Utrecht (The Netherlands), and Peter Giere, Institut für Systematische Zoologie, Museum für Naturkunde, Berlin (Germany) kindly lent us the Hubrecht collection of serially sectioned premetamorphic and metamorphic stages of *Discoglossus pictus*. Sebastien Steyer kindly helped to prepare the 3D models of DP FNSP 6582, and Corwin Sullivan improved some parts of the text linguistically. Additionally we thank an anonymous reviewer for his(her) constructive comments. We acknowledge the European Synchrotron Radiation Facility for the provision of synchrotron radiation facilities through the proposal (EC-850) and in particular the staff of ID17. The project was supported by the Geological Institute of the Czech Academy of Sciences (RVO67985831) to Zbyněk Roček and by St. Petersburg State University (Russia) (award No. 0.38.292.2015) to Natalia Baleeva.

REFERENCES

Barry T. H. (1956), "The ontogenesis of the sound-conducting apparatus of *Bufo angusticeps* Smith.," *Morphol. Jahrb.*, **97**, 477 – 544.

Bemis W. E. and Northcutt R. G. (1991), "Innervation of the basicranial muscle of *Latimeria chalumnae*," *Env. Biol. Fish*, **32**, 147 – 158.

Bernasconi A. F. (1951), "Über den Ossificationsmodus bei *Xenopus laevis* Daud.," *Mem. Soc. Helvet. Sci. Nat.*, **79**, 191 – 252.

Bickford D., Iskandar D., and Barlian A. (2008), "A lungless frog discovered on Borneo," *Curr. Biol.*, **18**, R374 – R375. http://dx.doi.org/10.1016/j.cub.2008.03.010

Blackburn D. C., Bickford D. P., Diesmos A. C., Iskandar D. T., and Brown R. M. (2010), "An ancient origin for the enigmatic Flat-Headed Frogs (Bombinatoridae: *Barbourula*) from the Islands of Southeast Asia," *PLoS ONE*, **5**, e12090. doi: 10.1371/journal.pone.0012090.

Boistel R., Aubin T., Cloetens P., Langer M., Gillet B., Josset P., Pollet N., and Herrel A. (2011a), "Whispering to the deaf: communication by a frog without external vocal sac or tympanum in noisy environments," *PLoS ONE*, **6**, e22080. doi: 10.1371/journal.pone.0022080

Boistel R., Pollet N., Tinevez J.-Y., Cloetens P., and Schlenker M. (2009), "Irradiation damage to frog inner ear during synchrotron radiation tomographic investigation," *J. Electron. Spectrosc. Relat. Phenom.*, **170**, 37 – 41.

Boistel R., Swoger J., Kržič U., Fernandez V., Gillet B., and Reynaud E. G. (2011b), "The future of three-dimensional microscopic imaging in marine biology," *Marine Ecol.*, **32**, 438 – 452.

Bolkay S. J. (1919), "Osnove uporedne osteologije anurskih batrahija sa dodatkom o porijeklu Anura i sa skicom naravnoga sistema istih," *Glas. Zemalj. Muz. Bosn. Herceg.*, **31**, 277 – 353.

Boy J. A. (1978), "Die Tetrapodenfauna (Amphibia, Reptilia) des saalpfälzischen Rotliegenden (Unter-Perm); SW-Deutschland). 1. Branchiosaurus," *Mainzer geowiss. Mitt.*, **7**, 27 – 76.

Bradley O. C. (1933), "M. retractor bulbi (oculi) in Carnivora and Ungulata," *J. Anat.*, **68**, 65 – 74.

Cannatella D. C. (1985), *Phylogeny of Primitive Frogs (Archaeobatrachians). Ph.D. Thesis*, The University of Kansas.

Carroll R. L. and Holmes R. (1980), "The skull and jaw musculature as guides to the ancestry of salamanders," *Zool. J. Linn. Soc.*, **68**, 1 – 40.

Castanet J., Meunier F., and Ricqlès A. (1977), "L'enregistrement de la croissance cyclique par le tissu osseux chez les vertébrés poïkilothermes: données comparatives et essai de synthèse," *Bull. Biol. Fr. Belg.*, **111**, 183 – 202.

Castanet J. and Smirina E. (1990), "Introduction to the skeletochronological method in amphibians and reptiles," *Ann. Sci. Nat. Zool. Paris*, **11**, 191 – 196.

Chilingaryan S., Mirone A., Hammersley A., Ferrero C., Helfen L., Kopmann A., dos Santos R., and Vagovic P. (2011), "A GPU-Based Architecture for Real-Time Data Assessment at Synchrotron Experiments," *IEEE Trans. Nucl. Sci.*, **58**, 1447 – 1455.

Clarke B. T. (1987), "A description of the skeletal morphology of *Barbourula* (Anura: Discoglossidae), with comments on its relationships," *J. Nat. Hist.*, **21**, 879 – 891.

Clarke B. T. (2007), "Comparative morphology and amphibian taxonomy: An example from the osteology of discoglossoid frogs," in: H. Heatwole and M. Tyler (eds.), *Amphibian Biology. Amphibian Systematics*, Surrey Beatty and Sons, Chipping Norton, Australia, pp. 2465 – 2612.

Corning H. K. (1902), "Über die vergleichende Anatomie der Augenmuskulatur," *Morphol. Jahrb.*, **29**, 94 – 140.

Cuvier G. (1824), *Recherches sur les ossements fossiles 5. 2ème partie. Ossemens de Reptiles. Résumé General. Nouvelle edition*, G. Dufour and Ed. d'Ocagne, Paris.

De Jongh H. J. (1968), "Functional morphology of the jaw apparatus of larval and metamorphosing *Rana temporaria* L.," *Neth. J. Zool.*, **18**, 1 – 103.

de Villiers C. G. S. (1934), "Studies on the cranial anatomy of *Ascaphus truei* Stejneger, the American "Liopelmid," *Bull. Mus. Comp. Zool.*, **71**, 1 – 38.

Diogo R. (2008), "Comparative anatomy, homologies and evolution of mandibular, hyoid and hypobranchial muscles of bony fish and tetrapods: a new insight," *Anim. Biol.*, **58**, 123 – 172. doi: 10.1163/157075608X328017

Diogo R., Hinits Y., and Hughes S. M. (2008), "Development of mandibular, hyoid and hypobranchial muscles in the zebrafish: homologies and evolution of these muscles within bony fishes and tetrapods," *BMC Dev. Biol.*, **8**, 24. doi: 10.1186/1471-213X-8-24.

Dong L., Roček Z., Wang Y., and Jones M. E. H. (2013), "Anurans from the Lower Cretaceous Jehol Group of Western Liaoning, China," *PLoS ONE*, **8**, e69723. doi: 10.1371/journal.pone.0069723

Duellman W. E. and Trueb L. (1986), *Biology of Amphibians*, McGraw-Hill Book Company, New York.

Edgeworth F. H. (1911), "On the morphology of the cranial muscles in some Vertebrates," *Quart. J. Micr. Sci.*, **222**, 167 – 316.

Edgeworth F. H. (1935), *The Cranial Muscles of vertebrates*, Cambridge Univ. Press, Cambridge.

Esteban M., Garcia-Paris M., and Castanet J. (1996), "Use of bone histology in estimating the age of frogs (*Rana perezi*) from a warm temperate climate area," *Can. J. Zool.*, **74**, 1914 – 1921.

Estes R. (1977), "Relationships of the South African fossil frog *Eoxenopoides reuningi* (Anura, Pipidae)," *Ann. S. Afr. Mus.*, **73**, 49 – 80.

Fabrezi M. and Chalabe T. (1997), "A review of the fusion of trigeminal and facial ganglia during larval development of some neobatrachian anurans," *Alytes*, **15**, 1 – 12.

Folie A., Rana R. S., Rose K. D., Sahni A., Kumar K., Singh L., and Smith T. (2013), "Early Eocene frogs from Vastan Lignite Mine, Gujarat, India," *Acta Palaeontol. Pol.*, **58**, 511 – 524. doi: 10.4202/app.2011.0063

Ford L. S. and Cannatella D. C. (1993), "The major clades of frogs," *Herpetol. Monogr.*, **7**, 94 – 117.

Francillon H. (1979), "Étude expérimentale des marques de croissance sur les humerus et les femurs des tritons crêtés (*Triturus cristatus* Laurenti) en relation avec la détermination de l'âge individual," *Acta Zool. Stockholm*, **60**, 223 – 232.

Francis E. T. B. (1934), *The Anatomy of the Salamander*, The Clarendon Press, Oxford.

Gao K.-Q. and Wang Y. (2001), "Mesozoic anurans from Liaoning Province, China, and phylogenetic relationships

of archaeobatrachian anuran clades," *J. Vertebr. Paleontol.*, **21**, 460 – 476.

Gaupp E. (1896), *Anatomie des Frosches. 1. Lehre vom Skelet und vom Muskelsystem*, Friedrich Vieweg und Sohn, Braunschweig.

Gaupp E. (1899), *Anatomie des Frosches. 2. Lehre vom Nerven- und Gefässsystem*, Friedrich Vieweg und Sohn, Braunschweig.

Guarino F. M., Andreone F., and Angelini F. (1998), "Growth and longevity by skeletochronological analysis in *Mantidactylus microtympanum*, a rain-forest anuran from southern Madagascar," *Copeia*, **1998**, 194 – 198.

Guarino F. B., Angelini F., and Cammarota M. (1995), "A skeletochronological analysis of three syntopic amphibian species from southern Italy," *Amphibia–Reptilia*, **16**, 297 – 302.

Haas A. (2001), "Mandibular arch musculature of anuran tadpoles, with comments on homologies of amphibian jaw muscles," *J. Morphol.*, **247**, 1 – 33.

Hall J. A. and Larsen J. H. (1998), "Postembryonic ontogeny of the Spadefoot Toad, *Scaphiopus intermontanus* (Anura: Pelobatidae): Skeletal morphology," *J. Morphol.*, **238**, 179 – 244.

Hutchinson V. H. (2008) "Amphibians: lungs' lift lost," *Curr. Biol.*, **18**, R392.

Inger R. F. (1954), "Philippine Zoological Expedition 1946 – 1947. Systematics and Zoogeography of Philippine Amphibia," *Fieldiana Zool.*, **33**, 183 – 531.

Iordansky N. N. (1991), "[Jaw musculature and the problem of phylogenetic relations of the Lissamphibia]," *Zool. Zh.*, **70**, 50 – 62 [in Russian, with English summary].

Iordansky N. N. (1992), "Jaw muscles of the Urodela and Anura: some features of development, functions, and homology," *Zool. Jahrb. Anat.*, **122**, 225 – 232.

Iordansky N. N. (1996), "Evolution of the musculature of the jaw apparatus in the Amphibia," *Adv. Amphib. Res. Former Sov. Union*, **1**, 3 – 26.

Iskandar D. T. (1978), "A new species of *Barbourula*: First record of a discoglossid from Borneo," *Copeia*, **1978**, 564 – 566.

Iskandar D. T. (1995), "Note on the second specimen of *Barbourula kalimantanensis* (Amphibia: Anura: Discoglossidae)," *Raffles Bull. Zool.*, 43, 309 – 311.

Jarvik E. (1942), "On the structure of the snout of crossopterygians and lower gnathostomes in general," *Zool. Bidr. Uppsala*, **21**, 235 – 675.

Jarvik E. (1980), *Basic Structure and Evolution of Vertebrates. 1*, Acad. Press, London.

Johnston P. (2011), "Cranial muscles of the anurans *Leiopelma* hochstetteri and *Ascaphus truei* and the homologies of the mandibular adductors in Lissamphibia and other gnathostomes," *J. Morphol.*, **272**, 1492 – 1512.

Jones M. E. H., Evans S. E., and Sigogneau-Russell D. (2003), "Early Cretaceous frogs from Morocco," *Ann. Carnegie Mus.*, **72**, 65 – 97.

Jurgens J. D. (1971), "The morphology of the nasal region of Amphibia and its bearing on the phylogeny of the group," *Ann. Univ. Stellenbosch*, 46, 1 – 146.

Kleinenberg S. E. and Smirina E. M. (1969), "[A contribution to the method of age determination in amphibians]," *Zool. Zh.*, **48**, 1090 – 1094 [in Russian].

Kleinteich T. and Haas A. (2007), "Cranial musculature in the larva of the caecilian, *Ichthyophis kohtaoensis* (Lissamphibia: Gymnophiona)," *J. Morphol.*, **268**, 74 – 88.

Krasny A., Lutz S., Gramsch C., Diepenbruck S., and Schlamann M. (2011), "Accessory eye muscle in a young boy with external ophthalmoplegia," *Clin. Anat.*, **24**, 948 – 949.

Lai Y.-C., Lee T.-H., and Kam Y.-C. (2005), "A skeletochronological study on a subtropical, riparian ranid (*Rana swinhoana*) from different elevations in Taiwan," *Zool. Sci.*, **22**, 653 – 658.

Lande M. A. and Zadunaisky J. A. (1970), "The structure and membrane properties of the frog nictitans," *Int. Ophtalmol.*, **9**, 477 – 491.

Lebedkina N. S. (2004), "Evolution of the amphibian skull," *Adv. Amphib. Res. Former Sov. Union*, **9**, 1 – 260.

Leclair R., Jr. and Castanet J. (1987), "A skeletochronological assessment of age growth in the frog *Rana pipiens* (Amphibia, Anura) from southwestern Quebec," *Copeia*, **1987**, 361 – 369.

Levine R. P., Monroy J. A., and Brainerd E. L. (2004), "Contribution of eye retraction to swallowing performance in the northern leopard frog, *Rana pipiens*," *J. Exp. Biol.*, **207**, 1361 – 1368.

Loetters S., Van der Meijden A., Coloma L. A., Boistel R., Cloetens P., Ernst R., Lehr E., Veith M. (2011), "Assessing the molecular phylogeny of a near extinct group of vertebrates: the Neotropical harlequin frogs (Bufonidae; *Atelopus*)," *Syst. Biodivers.*, **9**, 45 – 57.

Lubosch W. (1938) "Muskeln des Kopfes. C. Amphibien und Sauropsiden," in: L. Bolk, E. Göppert, E. Kallius, and W. Lubosch (eds.), *Handbuch der vergleichenden Anatomie der Wirbeltiere*, Urban & Schwarzenberg, Berlin, pp. 1025 – 1064.

Luther A. (1914), "Über die vom N. trigeminus versorgte Muskulatur der Amphibien," *Acta Soc. Sci. Fenn.*, **44**, 1 – 151.

Mao M., Huang Y., Mi Z., Liu Y., and Zhou C. (2012), "Skeletochronological study of age, longevity and growth in a population of *Rana nigromaculata* (Amphibia: Anura) in Sichuan, China," *Asian Herpetol. Res.*, **3**, 258 – 264.

Millot J. and Anthony J. (1965), *Anatomie de* Latimeria chalumnae. *II. Système nervaux et organes des sens*, Centre National de la Recherche Scientifique, Paris.

Myers G. S. (1943), "Rediscovery of the Philippine discoglossid frog, *Barbourula busuangensis*," *Copeia*, **1943**, 148 – 150.

Neal H. V. (1918), "The history of the eye muscles," *J. Morphol.*, **30**, 433 – 453.

Nevo E. (1968), "Pipid frogs from the Early Cretaceous of Israel and pipid evolution," *Bull. Mus. Comp. Zool.*, **136**, 255 – 318.

Pancharatna K. and Deshpande S. A. (2003), "Skeletochronological data on age, body size and mass in the Indian cricket frog *Limnonectes limnocharis* (Boie, 1835) (Anura: Ranidae)," *Herpetozoa*, **16**, 41 – 50.

Pancharatna K. and Kumbar S. M. (2005), "Estimation of age and longevity of the Indian Bullfrog *Hoplobtrachus tigerinus* (Daudin, 1802): A skeletochronological study," *Herpetozoa*, **18**, 147 – 153.

Přikryl T., Aerts P., Havelková P., Herrel A., and Roček Z. (2009), "Pelvic and thigh musculature in frogs (Anura) and origin of anuran jumping locomotion," *J. Anat.*, **214**, 100 – 139.

Pusey H. K. (1938), "Structural changes in the anuran mandibular arch during metamorphosis, with reference to *Rana temporaria*," *Quart. J. Micr. Sci.*, **80**, 479 – 551.

Pusey H. K. (1943), "On the head of the liopelmid frog, *Ascaphus truei*. I. The chondrocranium, jaws, arches, and muscles of a partly-grown larva," *Quart. J. Micr. Sci.*, **84**, 105 – 185.

Pyron R. A. and Wiens J. J. (2011), "A large-scale phylogeny of Amphibia including over 2800 species, and a revised classification of extant frogs, salamanders, and caecilians," *Mol. Phylogen. Evol.*, **61**, 543 – 583.

Rage J. C. and Dutheil D. B. (2008), "Amphibians and Squamates from the Cretaceous (Cenomanian) of Morocco. A preliminary study, with description of a new genus of pipid frog," *Palaeontogr. Abt. A*, **285**, 1 – 22.

Rage J.-C. and Roček Z. (1989), "Redescription of *Triadobatrachus massinoti* (Piveteau, 1936) an anuran amphibian from the early Triassic," *Palaeontogr. Abt. A*, **206**, 1 – 16.

Ramaswami L. S. (1937), "The morphology of the bufonid head," *Proc. Zool. Soc. London*, **1936**, 1157 – 1169.

Ramaswami L. S. (1940), "Some aspects of the chondrocranium in the tadpoles of south Indian frogs," *J. Mysore Univ. B*, **1**, 15 – 41.

Reiss J. O. (1997), "Early development of chondrocranium in the tailed frog, *Ascaphus truei* (Amphibia: Anura): Implications for anuran palatoquadrate homologies," *J. Morphol.*, **231**, 63 – 100.

Renier M., Fiedler S., Nemoz C., Gonzalez H., Berruyer G., and Bravin A. (2005), "A mechanical chopper with continuously adjustable duty cycle for a wide x-ray beam," *Nucl. Instrum. Meth. A*, **548**, 111 – 115.

Roček Z. (1981), "Cranial anatomy of frogs of the family Pelobatidae Stannius, 1856, with outlines of their phylogeny and systematics," *Acta Univ. Carol. Biol.*, **1980**, 1 – 164.

Roček Z. (2003), "Larval development and evolutionary origin of the anuran skull," in: H. Heatwole and M. Davies (eds.), *Amphibian Biology. Vol. 5. Osteology*, Surrey Beatty & Sons, Chipping Norton, pp. 1877 – 1995.

Roček Z. (2008), "The Late Cretaceous frog Gobiates from Central Asia: its evolutionary status and possible phylogenetic relationships," *Cret. Res.*, **29**, 577 – 591.

Roček Z., Eaton J. G., Gardner J., and Přikryl T. (2010), "Evolution of anuran assemblages in the Late Cretaceous of Utah, USA," *Palaeobio Palaeoenv.*, 90, 341 – 393. doi: 10.1007/s12549 – 010 – 0040 – 2

Roček Z. and Van Dijk E. (2006), "Patterns of larval development in Cretaceous pipid frogs," *Acta Palaeontol. Pol.*, **51**, 111 – 126.

Roček Z. and Nessov L. A. (1993), "Cretaceous anurans from central Asia," *Palaeontogr. Abt. A*, **226**, 1 – 54.

Roček Z., Wang Y., and Dong L. (2012), "Post-metamorphic development of Early Cretaceous frogs as a tool for taxonomic comparisons. *J. Vertebr. Paleontol.*, **32**, 1285 – 1292.

Sanchiz B. (1984), "Análisis filogenético de la tribu Alytini (Anura, Discoglossidae) mediante el estudio de su morfoestructura ósea," in: H. Hemmer and J. P. Alcover (eds.), *Life History of the Mallorcan Midwife Toad*, Editorial Moll, Ciutat de Mallorca, pp. 61 – 108.

Sanchíz B. and Schleich H. H. (1986) "Erstnachweis der Gattung *Bombina* (Amphibia: Anura) in Untermiozän Deutschlands," *Mitt. Bayer Staatssamm. Paläontol. Hist. Geol.*, **26**, 41 – 44.

Säve-Söderbergh G. (1936), "On the morphology of Triassic stegocephalians from Spitsbergen, and the interpretation of the endocranium in the Labyrinthodontia," *K. Sven. Vetensk. Handl. Ser. III*, **16**, 1 – 180.

Säve-Söderbergh G. (1945), "Notes on the trigeminal musculature in non-mammalian tetrapods," *Nov. Acta Reg. Soc. Sci. Uppsala Ser. 4*, **13**, 5 – 59.

Schlosser G. and Roth G. (1995), "Distribution of cranial and rostral spinal nerves in tadpoles of the frog *Discoglossus pictus* (Discoglossidae)," *J. Morphol.*, **226**, 189 – 212.

Schoch R. (1992), "Comparative ontogeny of early Permian branchiosaurid amphibians from southwestern Germany: Developmental stages," *Palaeontogr. Abt. A*, **222**, 43 – 83.

Shishkin M. A. (1973), *The Morphology of the Early Amphibia and Some Problems of the Lower Tetrapod Evolution*, Nauka, Moscow [in Russian].

Slabbert G. K. (1945), "Contributions to the cranial morphology of the European anuran *Bombina variegata* (Linné)," *Ann. Univ. Stellenbosch*, **23**, 67 – 89.

Smirina E. M. (1972), "[Annual layers in bone of *Rana temporaria*]," *Zool. Zh.*, **51**, 1529 – 1534 [in Russian].

Smirina E. M. (1994), "Age determination and longevity in amphibian," *Gerontology*, **40**, 133 – 146. doi: 10.1159/000213583

Smirina E. M. and Makarov A. N. (1987), "[On ascertainment of accordance between the number of layers in tubular bone of amphibians and the age of individuals]," *Zool. Zh.*, **66**, 599 – 604 [in Russian].

Sokol O. M. (1975), "The phylogeny of anuran larvae: a new look," *Copeia*, **1975**, 1 – 23.

Sokol O. M. (1977), "A subordinal classification of frogs (Amphibia: Anura)," *J. Zool. Lond.*, **182**, 505 – 508.

Spemann H. (1898), "Ueber die erste Entwicklung der Tuba Eustachii und des Kopfskelettes von *Rana temporaria*," *Zool. Jahrb.*, **11**, 389 – 416.

Špinar Z. (1972), *Tertiary Frogs from Central Europe*, Academia, Prague.

Stephenson E. M. (1951), "The anatomy of the head of the New Zealand frog, *Leiopelma*," *Trans. Zool. Soc. Lond.*, **27**, 255 – 305.

Suortti P., Fiedler S., Bravin A., Brochard T., Mattenet M., Renier M., Spanne P., Thomlinson W., Charvet A. M., Elleaume H., Schulze-Briese C., and Thompson A. C. (2000), "Fixed-exit monochromator for computed tomography with synchrotron radiation at energies 18 – 90 keV," *J. Synchrotron Rad.*, **7**, 340 – 347. doi: 10.1107/S0909049500008384

Swanepoel J. H. (1970), "The ontogenesis of the chondrocranium and of the nasal sac of the microhylid frog *Breviceps adspersus pentheri* Werner," *Ann. Univ. Stellenbosch*, **45**, 1 – 119..

Taylor E. H. and Noble G. K. (1924), "A new genus of discoglossid frogs from the Philippine Islands," *Am. Mus. Novitates*, **121**, 1 – 4.

Trueb L. (1973), "Bones, frogs, and evolution," in: J. L. Vial (ed.), *Evolutionary Biology of the Anurans*, Univ. of Missouri Press, Columbia, pp. 65 – 132.

van der Westhuizen C. M. (1961), "The development of the chondrocranium of *Heleophryne purcelli* Sclater with special reference to the palatoquadrate and the sound-conducting apparatus," *Acta Zool. Stockholm*, **42**, 1 – 72.

van Eeden J. A. (1951), "The development of the chondrocranium of *Ascaphus truei* Stejneger with special reference to the relations of the palatoquadrate to the neurocranium," *Acta Zool. Stockholm*, **32**, 42 – 124.

Wake D. B. and Castanet J. (1995), "A skeletochronological study of growth and age in relation to adult size in a population of plethodontid salamander *Batrachoseps attenuatus*," *J. Herpetol.*, **29**, 60 – 65.

Whitnall S. E. (1911), "An instance of the retractor bulbi muscle in man," *J. Anat. Physiol.*, **45**, 36 – 40.

Winkler D. A, Murry P. A., and Jacobs L. L. (1989), "Vertebrate paleontology of the Trinity Group, Lower Cretaceous of central Texas," in: D. A. Winkler, P. A. Murry, and L. L. Jacobs (eds.), *Field Guide to the Vertebrate Paleontology of the Trinity Group*, *Lower Cretaceous of Central Texas*, *Dallas*, Institute for the Study of Earth and Man, Southern Methodist University, Dallas, pp. 1 – 22.

Wu Y., Wang Y., and Hanken J. (2012), "Comparative osteology of the genus *Pachytriton* (Caudata: Salamandridae) from Southeastern China," *Asian Herpetol. Res.*, **3**, 83 – 102. doi: 10.3724/SP.J.1245.2012.00083